Electrochemical oxidation of anti-inflammatory drug meloxicam and its determination using boron doped diamond electrode

Renáta Šelešovská,[a*] Frederika Hlobeňová,[a] Jana Skopalová,[b] Petr Cankař,[c] Lenka Janíková,[a] Jaromíra Chýlková,[a]

[a] *University of Pardubice, Faculty of Chemical Technology, Institute of Environmental and Chemical Engineering, Studentská 573, 532 10 Pardubice, Czech Republic*

[b] *Department of Analytical Chemistry, Faculty of Science, Palacký University in Olomouc, 17. listopadu 12, 771 46 Olomouc, Czech Republic*

[c] *Department of Organic Chemistry, Faculty of Science, Palacký University in Olomouc, 17. listopadu 12, 771 46 Olomouc, Czech Republic*

** e-mail: renata.selesovska@upce.cz*

Abstract

Voltammetric behavior of a nonsteroidal anti-inflammatory drug meloxicam was firstly studied using boron doped diamond electrode (BDDE). Two irreversible anodic current peaks were observed in wide pH range at potentials +900 mV and + 1400 mV vs. saturated silver-silver chloride electrode. Mechanism of the electrochemical oxidation was proposed and confirmed using high performance liquid chromatography/mass spectrometry analysis of electrolyzed meloxicam solutions. Subsequently, an analytical method for meloxicam determination was developed using differential pulse voltammetry in connection with BDDE. This method provides low limit of detection (5.9×10^{-8} mol L^{-1}) and wide linear dynamic range (2.5×10^{-7}-8.5×10^{-5} mol L^{-1}). Finally, model solutions as well as pharmaceutical preparations were successfully analyzed, and the meloxicam content was determined.

Key words

Meloxicam, Voltammetry, Oxidation, Boron-doped diamond electrode, Pharmaceutical samples

1 Introduction

Meloxicam (MLX, 4-hydroxy-2-methyl-*N*-(5-methyl-1,3-thiazol-2-yl)-2*H*-1,2-benzothiazine-3-carboxamide-1,1-dioxide, Scheme 1) is a nonsteroidal anti-inflammatory drug from the oxicam class (NSAID). Oxicams are a group of structurally closely related substances which are widely used in the treatment of both acute and chronic pain syndromes of various origins, especially vertebrogenic and joint pain. They are also applied for short-term treatment of postoperative and post-traumatic pain. In general, their analgesic, anti-inflammatory and antipyretic effects are used. They are also widely utilized in some types of headaches [1]. MLX is indicated especially for the treatment of rheumatoid arthritis, osteoarthritis and other joint diseases [2-4]. Due to its very low solubility in acidic environment, it can cause only few local gastrointestinal side effects [5-8]. MLX was also associated with an increased risk of serious cardiovascular adverse events [8-10].

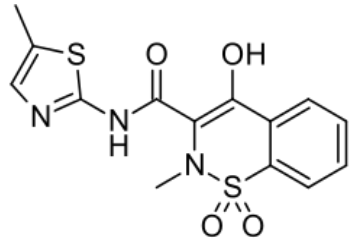

Scheme 1 Chemical structure of meloxicam.

MLX can be determined using various instrumental methods. High-performance liquid chromatography is most commonly used, *e.g.* in combination with diode or photodiode array detector [11, 12], UV spectrophotometric detector [13-16], or with mass spectrometer [17-20]. Method for separation and determination of MLX by thin-layer chromatography with densitometric detection was also described [21]. UV-VIS spectrophotometry [22-26] or fluorimetry [26, 27] represent another options for MLX determination. As an alternative, flow-injection chemiluminiscence determination can be also used [28]. These methods are

usually very sensitive and selective, but often require complex sample preparation for analysis and are time-consuming and instrumentally demanding. Because MLX is an electrochemically active compound, voltammetry offers a cheap, fast and simple alternative to the above mentioned methods.

In the first instance, reduction of MLX was utilized for its determination by single sweep oscillopolarography [29] and polarography [30] using dropping mercury electrode (DME). Hanging mercury drop electrode (HMDE) was used for MLX determination applying cathodic adsorptive stripping square wave voltammetry [31] as well as cathodic adsorptive striping differential pulse voltammetry [32]. The authors found that MLX provides two reduction signals on mercury electrode and Beltagi *et al.* [32] proposed the reduction mechanism of MLX. According to them, the first reduction step may be assigned to the reduction of the double bond in the enol form, while the second reduction step may correspond to the reduction of the carbonyl group of the keto form, to yield a saturated dihydrogen derivative. Radi *et al.* [33] studied the oxidative voltammetric behavior of meloxicam at a carbon paste electrode (CPE) and developed method for its determination using linear-scan voltammetry. According the authors, MLX gave rise to two voltammetric peaks, when the first one corresponds to the oxidation of amide functional group and the second one to the oxidation of enol functional group, respectively. Other published methods for MLX determination via its electrochemical oxidation used variously modified carbon based working electrodes. Wang *et al.* described method applying glassy carbon electrode (GCE) modified with anionic layer of cysteic acid providing electrostatic accumulation of the analyte onto the electrode surface [34]. MLX was also successfully determined at a poly-L-lysine (PLL)/carboxylated graphene oxide (GO–COOH)/modified glassy carbon electrode (GCE) [35], carbon paste electrode modified by molecularly imprinted polymer nanoparticle-multiwall carbon nanotubes [36], or graphene nanoparticles modified CPE [37]. A substantial

part of the last mentioned article is also devoted to the mechanism of MLX oxidation. In contrast to the mechanism reported in [33], the oxidation of the enol group is presumed to give rise to the first anodic signal and the oxidation of the amide group the second current response.

In the present work, MLX oxidation was firstly studied using boron doped diamond electrode (BDDE) [38-41]. This working electrode provide the number of advantages over traditionally employed electrodes, namely extreme hardness, high corrosion resistance, chemical inertness, high thermal conductivity, low sensitivity to dissolved oxygen, electrochemical stability in both alkaline and acidic media, very low and stable background current, and especially a wide usable potential window as well as a resistance to the electrode surface passivation [42-49]. These exceptional properties make it widely used in electroanalytical measurements in the determination of a number of biologically active substances and significant environmental contaminants as stated in various review articles [45, 50-52]. A number of studies related to drug determination were also described in the literature [53-59]. An oxidation mechanism of MLX was studied in more detail to clarify contradictory results reported in literature [33, 37]. The mechanism hitherto published was proposed based only on the results of pH effects on peak potential and peak current in cyclic voltammograms. Within our study, controlled potential electrolysis and ultraperformance liquid chromatography – mass spectrometry (UPLC/MS) with electrospray ionization (ESI) were used for generation and identification of products of MLX anodic oxidation. Finally, voltammetric method for MLX determination with BDDE was developed and utilized for analysis of a commercially available pharmaceutical preparation.

2 Experimental

2.1 Chemicals

Standard solution of 0.001 mol L^{-1} MLX (Sigma-Aldrich) was prepared by dissolution of the suitable amount in acetonitrile (Penta-Švec, Czech Republic). It was stored in a refrigerator at the temperature about +4°C and without light access. More dilute solutions were prepared fresh daily by dilution with supporting electrolyte. Britton-Robinson buffer (BRB) formed by acidic (0.4 mol L^{-1} H_3PO_4, H_3BO_3, and CH_3COOH, all from Penta-Švec, Czech Republic) and alkaline component (0.2 mol L^{-1} NaOH, Lachema, Czech Republic) was used as a supporting electrolyte. The solution of HNO_3 (pH 1) was diluted from 65 % HNO_3 (Penta-Švec, Czech Republic). The standard solutions of the other oxicams (Sigma-Aldrich), namely piroxicam (PRX), lornoxicam (LRX), and tenoxicam (TNX), were prepared by the same way as in case of MLX. Pharmaceutical preparation "Meloxicam Mylan 15 mg" originated from Generics (UK) Ltd, Great Britain.

2.2 Instrumentation

Voltammetric measurements were performed with Eco-Tribo Polarograph (Polaro-Sensors, Czech Republic) equipped with software POLAR.PRO version 5.1. The electrochemical cell was in a three-electrode arrangement. BDDE (Windsor Scientific, Great Britain, active surface area of 7.07 mm^2, inner diameter of 3 mm, resistivity of 0.075 Ω cm with a B/C ratio during deposition 1000 ppm) served as a working electrode, saturated argentchloride electrode (Ag/AgCl/KCl) was used as a reference and platinum wire as an auxiliary electrode (both Monokrystaly, Czech Republic). A potentiostat Autolab PGSTAT128 N (Metrohm Autolab, the Netherlands) was employed for linear sweep voltammetry (LSV) with rotating disc electrode (Autolab RDE, glassy carbon disc, diameter 0.5 cm) and controlled potential electrolysis with carbon fiber brush electrode (CFBE) [60]. Three-electrode system was completed with reference saturated calomel electrode (SCE) and platinum auxiliary electrode, which was placed in a cathodic compartment separated by a glass frit for bulk electrolysis.

Acquity UPLC system (Waters, USA) with PDA detector and mass spectrometric detector (QDA) equipped with heated electrospray ionization (HESI) and quadrupole analyzer were used for analysis of electrolyzed solutions. Potentiostat ADLC1 (Laboratorní přístroje, Czech Republic) with Model 5021A conditioning cell (ESA, Chelmsford, USA) containing porous graphite working electrode, Pd counter and a Pd/H_2 reference electrode, NE-1002X syringe pump (New Era Pump Systems, Farmingdale, USA) and Agilent 1100 Series LC/MSD Trap (Agilent Technologies, Palo Alto, USA) with electrospray ionization (ESI) were employed for on-line EC/MS experiments.

All measurements were carried out at laboratory temperature of 23±2 °C.

Values of pH were measured by pH-meter Accumet AB150 (Fisher Scientific, Czech Republic) and dissolution of standards as well as pharmaceutical samples was facilitated applying ultrasonic bath Bandelin Sonorex (Schalltec GmbH, Germany). Polishing kit (Electrochemical Detectors, Czech Republic) consisted of a polyurethane pad and Al_2O_3 powder (particle size 0.3 μm) was used for BDDE pretreatment.

Parameters of calibration curves and confidence intervals were calculated on the level of significance 0.05. Statistical parameters like limit of detection (LOD) and limit of quantification (LOQ) were calculated from the calibration dependences as 3× and 10×, respectively, of standard deviation of an intercept divided by a slope.

2.3 Procedures

2.3.1 Voltammetric measurements

Before beginning of the experiments, BDDE was activated and regenerated employing 20 cyclic voltammograms between initial potential (E_{in}) −1000 mV and switching potential (E_{switch}) +2200 mV directly in supporting electrolyte. Cycling was terminated at the positive potential values, *i.e.*, the final potential (E_{fin}) was +2200 mV. After this step, the working

electrode was ready for analysis. Between the particular measurements, no regeneration or activation step was inserted. This procedure ensured the O-terminated surface because BDD is easily oxidizable even by air oxygen.

Cyclic voltammetry (CV) was utilized for the investigation of the voltammetric behavior of MLX. If not defined otherwise, measurements were performed from E_{in} = −500 mV to E_{switch} = +2000 mV and back to −500 mV applying the scan rate (v) of 100 mV s^{-1}. In case of the scan rate study, the value of v varied from 25 to 500 mV s^{-1}. Considering very good sensitivity, differential pulse voltammetry (DPV) was used for the development of the method for MLX determination. BRB of pH 3 was chosen as a suitable supporting electrolyte. The optimized DPV parameters were as follows: E_{in} = 0 mV, E_{fin} = +2000 mV, v = 40 mV s^{-1}, pulse height +60 mV, and pulse width 20 ms (and another 20 ms as a current sampling time). The values of the peak height (I_p) were evaluated according to the baseline inserted as a tangent to the curve at minimum before and after the peak. Hydrodynamic voltammograms were recorded with RDE using LSV at scan rate 10 mV s^{-1} and rotation speed 500-3000 rpm (52–314 rad s^{-1}). Glassy carbon electrode disk was polished before each scan with alumina slurry (0.05 μm particle size) on microcloth (Buehler).

2.3.2. Controlled potential electrolysis, HPLC/MS analysis and EC/MS experiments

Carbon fiber brush electrode (CFBE) used as the working electrode for bulk electrolysis was prepared in the laboratory according to the previously described procedure [61]. Before use, CFBE was sonicated in acetonitrile and deionized water for 5 minutes. Subsequently, it was electrochemically pretreated in 0.1 mol L^{-1} H_2SO_4 using 50 potential cycles from -1.7 to +2.0 V (vs. SCE) and thoroughly washed with deionized water. Controlled potential electrolysis was performed with 4 mL of 5×10^{-4} mol L^{-1} MLX solution in the mixture of 0.2 mol L^{-1} aqueous CH_3COOH and CH_3CN (1/1, v/v) in anodic compartment of the electrolytic cell, at

potentials of 0.8 V and 1.2 V (vs. SCE) for 60 min on the electromagnetic stirrer. The cathodic compartment was filled with 0.2 mol L^{-1} CH_3COOH. Electrolyzed samples and respective standard solution of MLX were analyzed by UPLC/MS. Chromatographic separation was performed on XSelect HSS T3 column (3 mm × 50 mm, 2.5 μm, Waters) at 23 °C. Mobile phase consisted of 0.01M aqueous ammonium acetate (solvent A) and a mixture CH_3CN/H_2O (90/10, v/v, solvent B). Gradient elution: 0–5 min (0–55 % B), 5–10 min (55 % B) was performed with flow rate 0.6 mL min^{-1}. After the analysis the column was equilibrated with solvent A for 2.5 min. The injection volume was 5 μL. Mass spectrometry conditions were set for both positive (ESI+) and negative (ESI-) electrospray ionization modes as follows: capillary voltage 0.8 kV, cone 25 V, source temperature 120 °C, heated probe temperature 600 °C and the acquired mass range *m*/*z* 60–600.

In on-line EC/MS experiments, MLX solution (c = 5×10^{-5} mol L^{-1}) in 0.2 mol L^{-1} aqueous CH_3COOH and CH_3CN (1/1, v/v) was pumped through the coulometric cell to the electrospray ion source of MS by flow rate 8 μL min^{-1}. Potential of the working porous graphite electrode in the cell gradually increased from 0 to 0.7 V (vs. Pd/H_2) in steps of 20 mV. At each potential, MS signals were recorded for 60 s in both positive and negative ESI modes under the following conditions: drying gas (N_2), flow rate 5 L min^{-1}, drying temperature 180 °C, nebulizer pressure 15 psi, capillary voltage ±3.5 kV, end plate offset ±0.5 kV. Helium was used as collision gas. Data were processed using DataAnalysis 3.3 software (Bruker Daltonik, Germany).

2.3.3 Analysis of pharmaceutical sample

The stock solution for the quantitative experiments was prepared from one blister of MLX tablets of “Meloxicam Mylan 15 mg” containing 10 tablets with declared content of 15 mg MLX/Tbl. Tablets were powdered in a grinding mortar, and then the sample was

quantitatively transferred into a 1000 mL standard flask and was dissolved in acetonitrile applying the ultrasonic bath. This solution was filtered. The concentration of MLX in the prepared solution was about 4.27×10^{-4} mol L^{-1} (calculated according to the content of the substance declared by the producer). 35 µL of the sample solution was added to the polarographic cell with 15 mL of the supporting electrolyte (BRB pH 3) and the determination was carried out by the standard addition method and two standard additions (15 µL of 0.001 mol L^{-1} MLX) were applied at least. The determination was five times repeated and relative standard deviation of repeated determination (*RSD*) was calculated.

3 Results and discussion

3.1. Voltammetric behavior of meloxicam

Oxidation of MLX on BDDE was firstly measured in BRB (pH 3) at 100 mV s^{-1}. These conditions were taken from the literature [33]. The obtained cyclic voltammogram of 1.0×10^{-5} mol L^{-1} MLX is depicted in Fig. 1 (red curve). In accordance with the literature, MLX provided two oxidation signals at the potential values (E_p) of +900 and +1400 mV. No corresponding reduction peak was observed on the cathodic curve, suggesting an irreversible course of the ongoing electrode reaction. This finding was confirmed also during the measurements with different E_{switch} values as it is evident from the inset of Fig. 1.

According to the authors of the previous publication [33], the first MLX peak corresponds to the oxidation of amide function group and the second one to the oxidation of enol function. Eroglu *et al.* [37] assigned the first signal to the oxidation of enol group and the second one to the oxidation of amide. None of the research groups provided any evidence to support their proposal (*e.g.*, mass spectroscopy analysis of the products of electrolysis). Moreover, CV voltammograms of other oxicams (PRX, LRX, and TNX) were preliminary measured on the same BDDE and for comparison they are placed in Fig. 1 too. All these

compounds provide one oxidation signal at the same E_p as the first peak of MLX which predicts the same electrochemical process. In the literature [62, 63], this peaks are also assigned to the oxidation of enol group. In the following chapters we would like to clarify the oxidation mechanism of MLX among others using HPLC-MS technique.

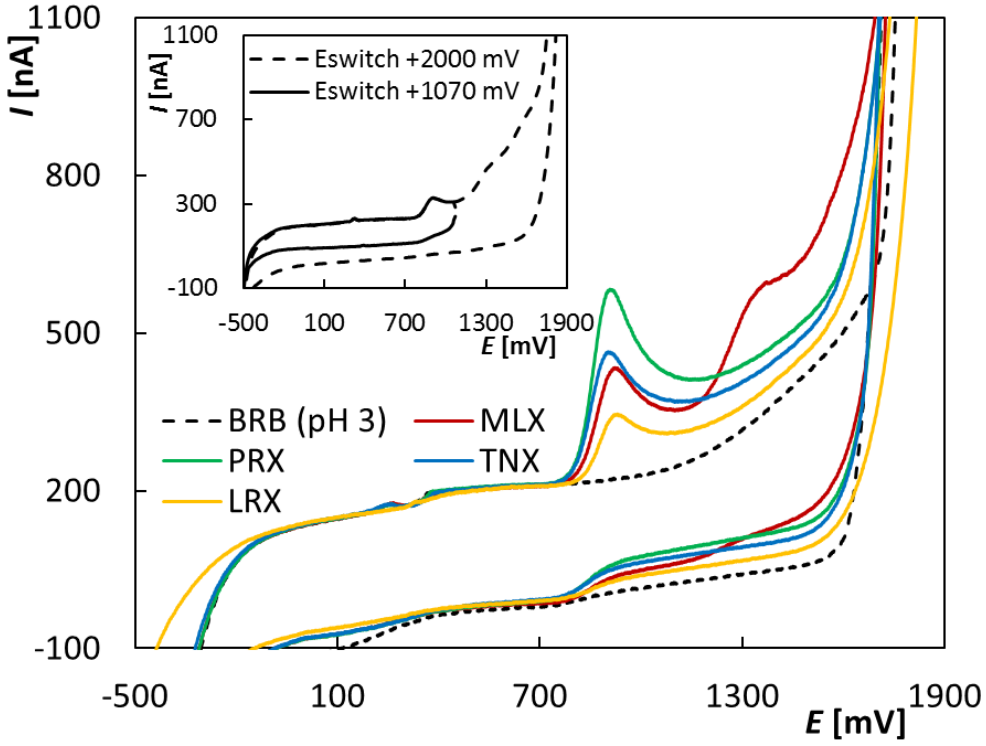

Figure 1 Cyclic voltammograms of oxicams in BRB (pH 3) obtained on BDDE; E_{in} = −500 mV, E_{switch} = +2000 mV, v = 100 mV s^{-1}, c_{MLX} = c_{PRX} = c_{LRX} = c_{TNX} = 1.0×10^{-5} mol L^{-1}; ***Inset:*** Cyclic voltammograms of MLX with E_{switch} = +2000 and +1070 mV.

3.1.1. Dependence on pH

Fig. 2 shows the influence of pH of supporting electrolyte in the range from 1 to 12 on MLX (1.0×10^{-5} mol L^{-1}) anodic signals obtained by CV (v = 100 mV s^{-1}). The acidic medium was ensured with the solution of diluted HNO_3, and other pH values (2-12) were reached using BRB. It is evident that the best developed two peaks were observed in acidic media (pH 1-3) and with the increasing of pH both signals decrease and widen. In alkaline electrolyte the first peak became very difficult evaluable and the second one disappeared. Due to the following

analytical usage, attention was paid especially to the first peak. Its position shifts to more negative potential values in the range of pH 1-3 and shows a shift in the opposite direction in more basic media (see the inset of Fig. 2). The peak height (I_p) reached maximum in acidic medium (pH 1-3) as it is documented in the inset of Fig. 2. Changes in trends of both I_p and E_p of the first MLX peak in the dependence on pH indicate the change in protolytic forms of MLX. As reported [64], MLX has two pK_a values: 1.09 and 4.18. At low pH values (<1.09), MLX exists mainly in the cation form, at pH > 4.18 the anion form prevail in aqueous solutions. The pH dependence of I_p and E_p shows that the anionic form of MLX is more difficult to oxidize than the protonated and uncharged form. BRB of pH 3 was applied as suitable supporting electrolyte for all next voltammetric measurements.

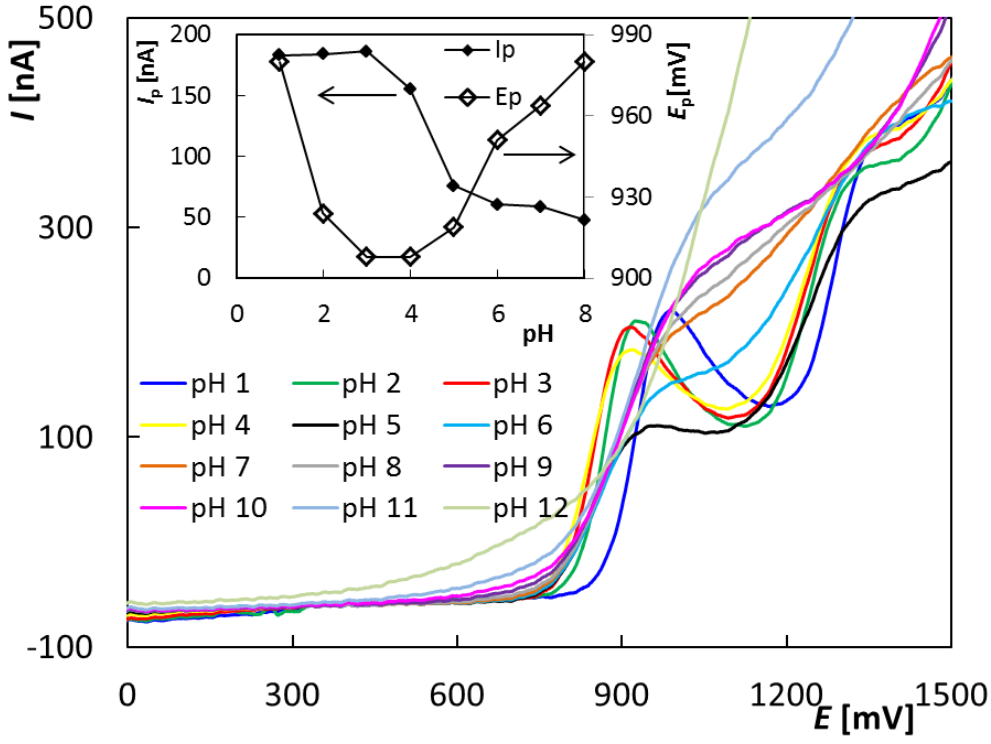

Figure 2 Anodic parts of cyclic voltammograms of MLX obtained on BDDE in dependence on pH; supporting electrolyte – solution of HNO_3 (pH 1) and BRB (pH 2-12), E_{in} = −500 mV, E_{switch} = +2000 mV, v = 100 mV s^{-1}, c_{MLX} = 1.0×10^{-5} mol L^{-1}; ***Inset:*** Dependence of I_p and E_p of the first oxidation peak on pH of supporting electrolyte.

3.1.2. Dependence on scan rate

The effect of scan rate on the voltammetric behavior of MLX can be useful for determining the controlling process and for proposing mechanism of the observed electrode reactions. CV voltammograms of MLX (1.0×10^{-5} mol L^{-1}) obtained in BRB (pH 3) on BDDE in dependence on v (50-450 mV s^{-1}) are shown in Fig. 3. It is evident that both anodic signals increased with growing v and simultaneously their E_p shifted to more positive potential values confirming the irreversible course of the oxidation reactions. While dependence of I_p on v for the first signal, that we are interested in (inset of Fig. 3), did not show a linear pattern, dependence of I_p on square root of v (I_p_$v^{1/2}$) was linear and can be described by equation (1) with the appropriate correlation coefficient. This indicates the diffusion-controlled process. It was verified also with logarithmic dependence (log(I_p)_log(v)) described by equation (2). The significant influence of kinetics was also proved because the value of slope lies below the theoretical value of 0.5.

$$I_p\ [\mathrm{nA}] = (38.5 \pm 2.1)\ (v\ [\mathrm{mV\ s^{-1}}])^{1/2} + (203 \pm 33),\ r = 0.9901 \quad (1)$$

$$\log\left(I_p\ [\mathrm{nA}]\right) = (0.368 \pm 0.011) \log\ (v\ [\mathrm{mV\ s^{-1}}]) + (2.030 \pm 0.028),\ r = 0.9963 \quad (2)$$

Consistent with the findings of the pH-dependency study, an increasing effect of kinetics with increasing pH was observed. While at pH 1 the slope of log(I_p)_log(v) (equation 3) is very close to the theoretical value of 0.5 for a pure diffusion-controlled process, at pH 5 (where the anionic form of MLX predominates) the slope value 0.31 (equation 4) is lower than at pH 3 (equation 2), showing that the influence of kinetics on the control process increases with pH.

$$\log\left(I_p\ [\mathrm{nA}]\right) = (0.4741 \pm 0.0088) \log\ (v\ [\mathrm{mV\ s^{-1}}]) + (1.425 \pm 0.020),\ r = 0.9991 \quad (3)$$

$$\log\left(I_p\ [\mathrm{nA}]\right) = (0.3110 \pm 0.0128) \log\ (v\ [\mathrm{mV\ s^{-1}}]) + (1.313 \pm 0.028),\ r = 0.9099 \quad (4)$$

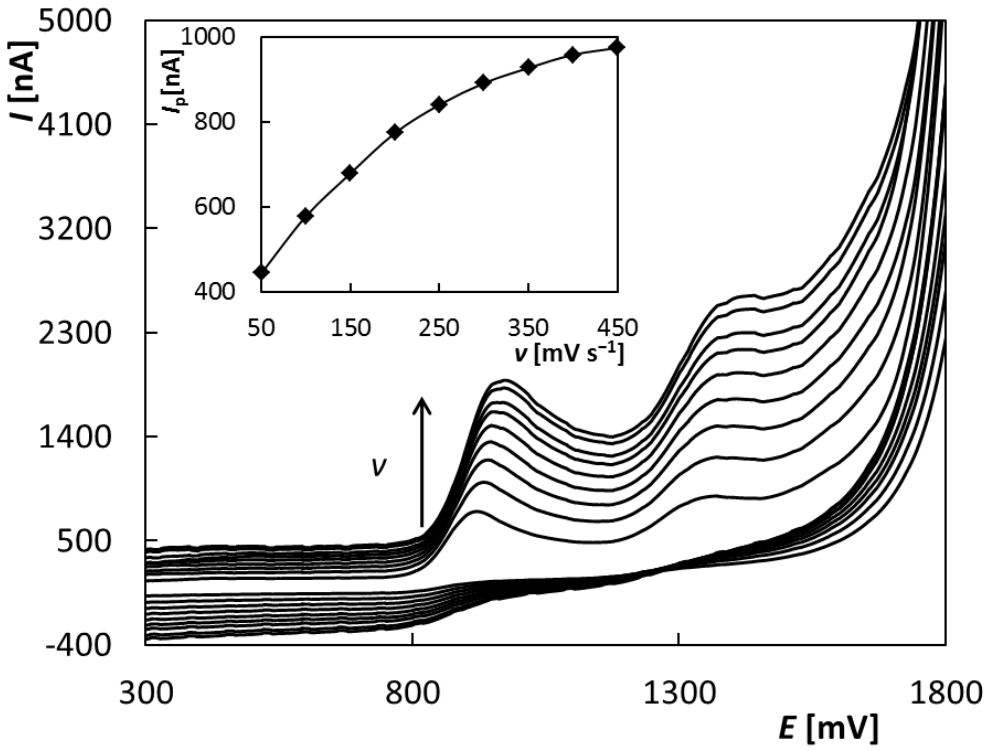

Figure 3 Cyclic voltammograms of MLX obtained on BDDE in dependence of scan rate; supporting electrolyte – BRB (pH 3), E_{in} = −500 mV, E_{switch} = +2000 mV, v = 50-450 mV s^{-1}, c_{MLX} = 1.0×10^{-5} mol L^{-1}; ***Inset:*** Dependence of I_p on pH of supporting electrolyte.

3.2. Oxidation mechanism

3.2.1. Number of exchanged electrons

Linear sweep voltammograms of MLX recorded on RDE at different rotation velocity were evaluated and used to estimate number of electrons transferred at anodic oxidation of MLX. As the electrochemical reaction evinced mixed diffusion-kinetic control, Koutecký-Levich equation (5) was used to calculate number of involved electrons from the slope of the dependence of $1/I$ on $1/\omega^{1/2}$ [65]:

$$\frac{1}{I} = \frac{1}{0.62nFAD_A^{2/3}\upsilon^{-1/6}c_A\omega^{1/2}} + \frac{1}{nFAk_hc_A}, \quad (5)$$

where I represents electrode current, n is number of electrons, F is the Faraday constant, A is area of the disc electrode (0.196 cm^2), υ is the kinematic viscosity of the solution (8.84×10^{-3} cm^2 s^{-1}), c_A - concentration of analyte (9.52×10^{-8} mol cm^{-3}), ω – rotating velocity (rad s^{-1}) and k_h – heterogenous rate constant (cm s^{-1}). Diffusion coefficient D_A of MLX was estimated from the Wilke-Chang equation (6) [66]:

$$D_A = 7.4 \times 10^{-8} \frac{T(xM)^{0.5}}{\eta V^{0.6}}, \quad (6)$$

where T is thermodynamic temperature, η is viscosity, x and M are association parameter and molar weight of the solvent, respectively, and V is molar volume of the solute. Under the respective experimental conditions T = 298.15 K, viscosity of 1:1 (v/v) acetonitrile – water mixture η = 0.801 cP [67], x = 2.6, M = 18.015 g mol^{-1} and molar volume of MLX V = 217.7±3.0 mL (calculated using ACD/ChemSketch software), the value of D_A = 0.746×10^{-5} cm^2 s^{-1} was obtained. Slopes of the dependence $1/I = f(1/\omega^{1/2})$ were evaluated from hydrodynamic voltammograms of MLX (Fig. S1-A, B in Supplementary information file) at 5 different potentials (0.8-1.0 V) and each value was used to calculate number of electrons with the result: n = 2.09±0.11. This result corresponds to the number of electrons n = 1.98 found by convolutive procedure [68] applied to linear sweep voltammogram recorded on a static disc electrode (see Fig. 2 in Supplementary material). It can be concluded, that the first step of the anodic oxidation of meloxicam is a two-electron process.

3.2.2. UPLC/MS analysis of oxidation products

The previously proposed mechanisms of electrochemical oxidation of MLX in aqueous solutions attribute the first oxidation step to either the amide function group [33] or the enol group [37]. Both hypotheses are based on the results of the voltammetric behavior of this substance and its similarity to the behavior of structurally related substances. In this work, we

attempted to elucidate the reaction mechanism based on UPLC/MS analysis of MLX electrolysis products produced on large-area CFBE. For comparison, on-line EC/MS experiments were performed with flow-through coulometric cell containing working porous graphite anode coupled to mass spectrometer with ion trap analyzer. In both types of experiments, 0.2 mol L^{-1} aqueous CH_3COOH with acetonitrile (1/1, v/v) was used to provide the appropriate acidic medium and to maintain MLX in solution. Potentials for the bulk electrolysis in the off-line experiment were selected from hydrodynamic voltammograms (Fig. S1-A in the Supplementary information file) at the limiting current of the first anodic wave and at the steep part of the second waves (to avoid formation of hydrogen bubbles in the narrow cathodic compartment at higher potentials).

UPLC/MS analysis of the standard MLX solution provided a single peak with retention time t_r = 4.62 min and protonated molecule $[M+H]^+$ at *m*/*z* 352 (Fig. S3a and S4a in the Supplementary information file, respectively). Fragmentation pattern of the spectrum acquired in ESI+ mode (Fig. S4a) with fragment ions at *m*/*z* 115, 141 and 184 corresponds to those reported in the literature [69] Mass spectrum recorded in ESI- mode (Fig. S4b) shows fragments at *m*/*z* 286 (loss of SO_2), *m*/*z* 210 and *m*/*z* 146 (loss of SO_2 from the fragment *m*/*z* 210).

Total ion current chromatogram of the MLX solution electrolyzed at potential of +0.8 V, corresponding to the limiting current of the first voltammetric wave of MLX, revealed four main peaks of reaction products (Fig. S3b in Supplementary information file). Two peaks with t_r = 4.30 min and t_r = 5.83 min and *m*/*z* 350 appertain to isomeric products with the *m*/*z* value two units lower than that of MLX. Mass spectra of these products are similar (Fig. S5) with common fragment ions at *m*/*z* 210 and *m*/*z* 141, which differ in their intensities. Presence of the fragment *m*/*z* 141 corresponding to the methyl-thiazolyl carboxamide moiety, which is characteristic of MLX, confirms that this part of the molecule

remain unchanged. The third peak with t_r = 5.32 min belongs to a product with $[M+H]^+$ at *m*/*z* 368 (Fig. S6a in the Supplementary information file). The main fragment at *m*/*z* 141 indicates presence of unchanged methyl-thiazolyl carboxamide moiety of the product. The fourth peak with t_r = 3.52 min, $[M+H]^+$ at *m*/*z* 171 (Fig. S6b in the Supplementary information file) rendered fragment ions at *m*/*z* 143 and *m*/*z* 115 corresponding to two consecutive losses of CO from two carbonyl groups in the product structure. These results indicate that all products of the first step of meloxicam oxidation have an unchanged methyl-thiazolyl carboxamide structure. Therefore, in the first step of the electrochemical reaction, oxidation occurs at the enol group of the hydroxybenzothiazine ring.

Chromatogram of the MLX solution electrolyzed at potential of +1.2 V corresponding to the steep part of the second oxidation wave of MLX, gave a peak with retention time t_r = 3.18 min and *m*/*z* 187 in ESI+ or *m*/*z* 185 in ESI- (Fig. S7 in the Supplementary information file). Fragments at *m*/*z* 143 and 141 formed by losses of CO_2 and HCOOH, respectively, confirm that the product is a carboxylic acid having unchanged methyl-thiazolyl carboxamide moiety (**9** in Scheme 2).

The products detected in the electrolyzed MLX solutions by UPLC/MS were also observed in on-line EC/MS experiments that may detect unstable reaction products. MS signal intensity of individual reaction products varied with the potential applied to the working electrode in accordance with the UPLC/MS analysis of MLX solutions electrolyzed at lower and higher potential (Fig. S8 in the Supplementary information file). In addition, in the mass spectra obtained at higher potentials of electrolysis, one more product was observed at *m*/*z* 296 in ESI+. Collision spectrum of this product (Fig. S9, Supplementary information file) gave major fragments at *m*/*z* 253 (loss of NCOH), *m*/*z* 235 (subsequent loss of H_2O) and *m*/*z* 210, corresponding to unchanged *N*-methyl benzothiazinone moiety. This product was found in UPLC/MS analysis only at very low content, indicating its low long-term stability.

However, this finding shows that the amide or methylthiazole group of MLX can be subjected to an electrochemical reaction at sufficiently high potential.

3.2.3. Reaction mechanism

Voltammetric experiments revealed that the electrochemical oxidation of MLX proceeds in two irreversible steps, preferably under acidic conditions. Based on the identified products of electrolysis performed at the limiting current of the first two-electron wave, the following reaction mechanism was proposed (Scheme 2): The electrode reaction starts with the electron transfer from the hydroxyl oxygen of the enol group. Deprotonation of the formed cation radical and subsequent transfer of the second electron leads to intermediate **2**, which is susceptible to form **3** by addition of water and its ring-chain tautomeric form **4**. Formation of the structure **3** is consistent with reaction mechanism proposed for electrochemical oxidation of a relative drug piroxicam [63]. Under acidic conditions, intramolecular condensation of **4** leads to benzoisothiazoliminium form **5**, which can be hydroxylated to give unstable intermediate **6**. Decomposition of **6** produces thiazole (**7**) and benzoisothiazole (**8**), the two main reaction products of the first electrochemical oxidation step of MLX. As the first reaction step starts with the electron withdrawing from the "enolic" hydroxyl, after its deprotonation at pH > pK_a (4.18) the electrode reaction becomes kinetically controlled by the rate of protonation of the deprotonated enolate.

Second step of the electrochemical oxidation includes most likely subsequent oxidation of aldehyde group of **7** to give the corresponding monoamide of oxalic acid (**9**). However, oxidation of the methylthiazole moiety to corresponding sulfone and sulfoxide [70] can also be supposed according to the results of EC/MS experiment. Hydrolytic cleavage of the sulfoxide can lead to formation of the detected product at *m*/*z* 296 in ESI+.

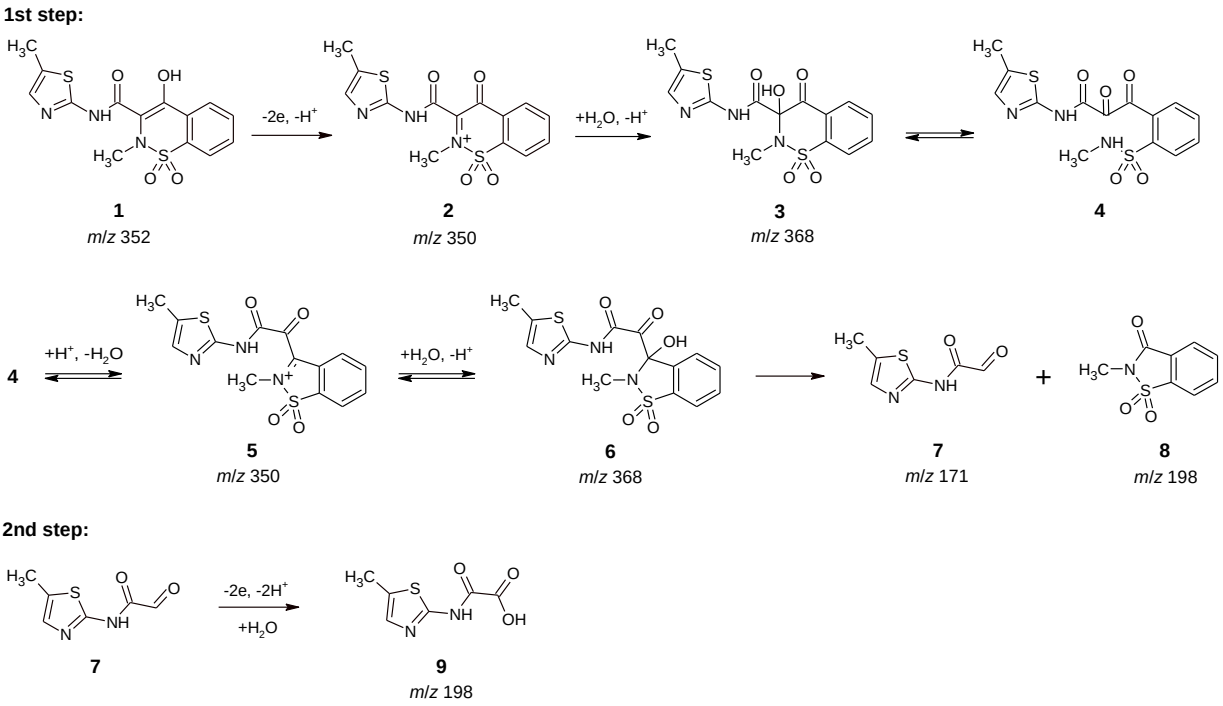

Scheme 2 Proposed mechanism of the first and second step of electrochemical reactions of meloxicam with mass-to-charge ratios in positive ion mode ESI-MS.

3.3. Voltammetric determination of meloxicam

3.3.1. Optimization of DPV parameters

DPV was applied for the development of voltammetric method for MLX determination and the first oxidation peak was used for this purpose. At the beginning, basic parameters of DPV like scan rate, pulse height and pulse width were optimized. All the following experiments were carried out in BRB of pH 3 and with the MLX concentration of 5.0×10^{-6} mol L^{-1} in a polarographic vessel. One parameter was always changed and the others were kept constant. Specific settings are described in the caption of the Fig. 4 which illustrates the courses of the particular dependences of I_p on the individual tested parameters. The value of v was changed from 10 to 100 mV s^{-1}. Fig. 4A shows the peak increased up to 40 mV s^{-1} and therefore this value was set for all the following measurements. The pulse height was tested in the range

from 10 to 100 mV. I_p increased approximately linearly in dependence of pulse height up to value 70 mV (Fig. 4B) but simultaneously at the higher values MLX oxidation signal was spreading. For further experiments, a pulse height of 60 mV was selected as a compromise between peak height and shape. The last examined parameter – pulse width was tested in the range of 10-100 ms (Fig. 4C) and the value of 30 ms was applied for all of the future experiments.

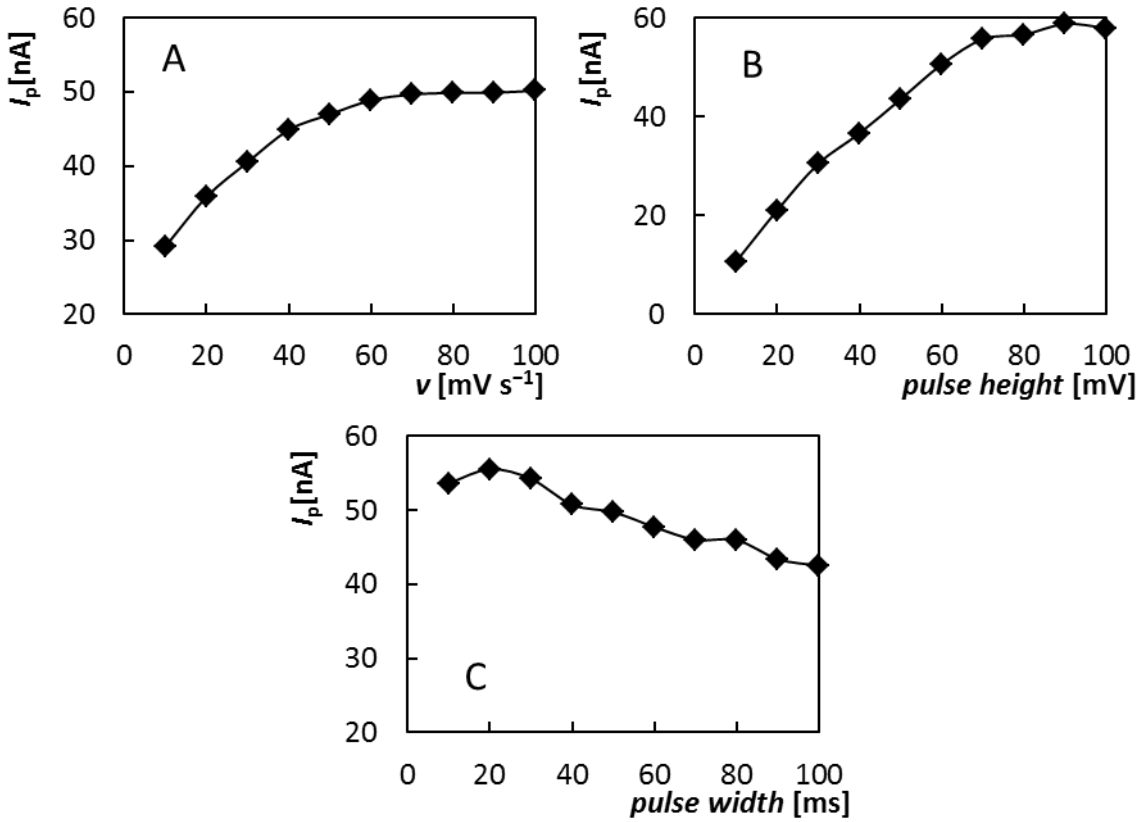

Figure 4 Dependences of I_p on v (A), I_p on pulse height (B), and I_p on pulse width (C) obtained on BDDE using DPV; supporting electrolyte – BRB (pH 3), E_{in} = 0 mV, E_{fin} = +2000 mV, v = 10-100 mV s^{-1} (A), and 40 mV s^{-1} (B, C), pulse height = +50 mV (A), +10-+100 mV (B), and +60 mV (C), pulse width = 50 ms (A, B), 10-100 ms (C), c_{MLX} = 5.0×10^{-6} mol L^{-1}.

Another factor, that significantly influences the electrochemical properties of BDDE surface and thus the height and shape of the measured current signals, is the pretreatment

procedure [71]. In case of MLX determination we tested four different pretreatment processes as follows: (i) anodic pretreatment (E = +2400 mV, t = 300 s), (ii) cathodic pretreatment (E = −2000 mV, t = 300 s), (iii) insertion of 20 cyclic voltammograms (E_{in} = −1000 mV, E_{switch} = E_{fin} = +2200 mV, v = 100 mV s^{-1}), and (iv) polishing on alumina. DPV voltammograms of MLX (5.0×10^{-6} mol L^{-1}) obtained under the optimized parameters always after the insertion of particular pretreatment procedure directly in analyzed solutions before scan are illustrated in Fig. 5. It is evident that the highest and the sharpest peaks were obtained similarly after cycling and anodic pretreatment that both provide O-terminated BDDE surface. On the other hand, the lowest signal was recorded after application of negative potential and reduction of the working surface, respectively (H-terminated surface). Concerning polishing, significant background increase and worsening of the repeatability of measurement was observed. Due to the better repeatability and slightly higher peak, CV was selected as suitable pretreatment procedure for all further measurements. Moreover, it was found that it is sufficient to include cycling only at the beginning of the work. There is no need to activate or regenerate the electrode surface between the individual measurements. The electrode passivation does not occur, which is confirmed by the obtained low value of relative standard deviation of 11 repeated measurements (RSD_{11} = 0.3 %) of 5.0×10^{-6} mol L^{-1} MLX.

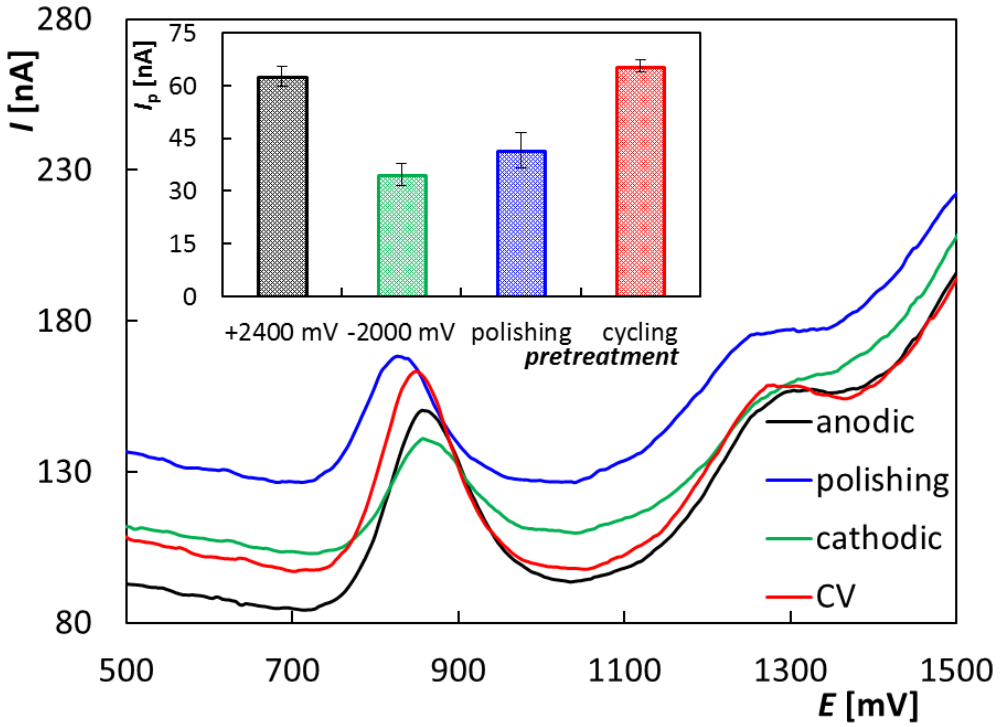

Figure 5 DPV voltammograms of 5×10^{-6} mol L^{-1} MLX obtained on BDDE after different pretreatment procedure; supporting electrolyte – BRB (pH 3), E_{in} = 0 mV, E_{fin} = +2000 mV, v = 40 mV s^{-1}, pulse height = +60 mV, pulse width = 30 ms, c_{MLX} = 5.0×10^{-6} mol L^{-1}; ***Inset:*** Dependence of I_p on applied pretreatment procedure: (i) anodic pretreatment – E = +2400 mV, t = 300 s, (ii) cathodic pretreatment – E = −1000 mV, t = 300 s, (iii) cycling – 20 cyclic voltammograms, E_{in} = −1000 mV, E_{switch} = E_{fin} = +2200 mV, v = 100 mV s^{-1}, (iv) polishing – in alumina.

3.3.2. Analysis of model solutions

New voltammetric method was applied to measurement of various concentration dependences of MLX in model solutions to determine the basic statistical parameters like linear dynamic range (*LDR*), *LOD*, and *LOQ*. In Fig. 6, an example of the recorded DPV voltammograms in dependence on MLX concentration in the range from 1.0×10^{-6} to 1.7×10^{-5} mol L^{-1} is shown. As it is obvious from the inset of this figure, I_p (peak 1) increased linearly with growing analyte concentration and the obtained dependence can be described by the equation (7) with

the corresponding correlation coefficient. Calculated statistical parameters are summarized in Table 1. The obtained value of *LOD* is very low (5.9×10^{-8} mol L^{-1}), especially considering the use of bare BDDE as working electrode. Our method was also compared with those published for MLX determination in literature. As it is obvious from Table 2, best results were obtained using adsorptive stripping voltammetry in connection with HMDE [31] or with carbon paste electrode modified by molecularly imprinted polymer nanoparticle-multiwall carbon nanotubes (MIP@MWCNT/CPE) [36]. On the other hand, BDDE provide significantly better value of *LOD* than bulk CPE [33]. The main advantage of BDDE in comparison with other presented modified electrodes [34-37] lies in better repeatability and stability of the electrode surface as well as in simple and time undemanding preparation of the electrode for measurement.

$$I_p\ [\text{nA}] = (12.370 \pm 0.089)\ c\ [\mu\text{mol L}^{-1}] - (0.64 \pm 0.91),\ r = 0.9995 \quad (7)$$

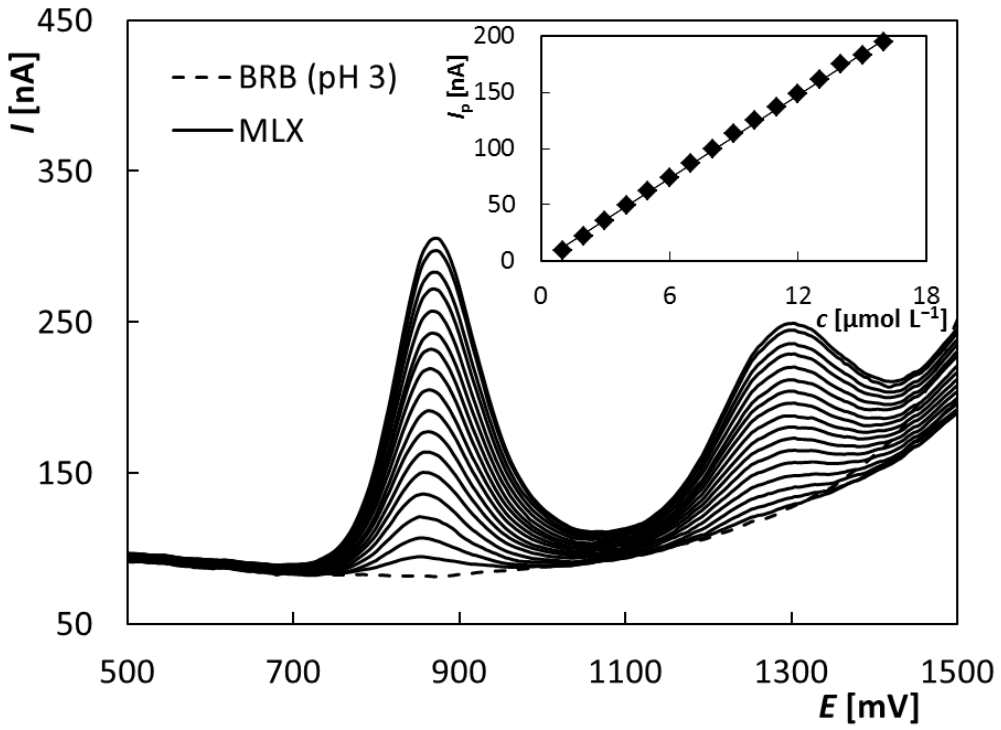

Figure 6 DPV voltammograms of MLX obtained on BDDE in dependence on concentration; supporting electrolyte – BRB (pH 3), E_{in} = 0 mV, E_{fin} = +2000 mV, v = 40 mV s^{-1}, pulse

height = +60 mV, pulse width = 30 ms, c_{MLX} = 1.0×10^{-6}-1.7×10^{-5} mol L^{-1}; ***Inset:*** Dependence of I_p on concentration of MLX.

Table 1 Statistical parameters for MLX determination

*LOD** [mol L^{-1}]	*LOQ** [mol L^{-1}]	*LDR* [mol L^{-1}]	RSD_{11}** [%]
5.9×10^{-8}	1.9×10^{-7}	2.5×10^{-7}-8.5×10^{-5}	0.3

*Calculated from the recorded concentration dependence in the range of 2.5×10^{-7}-1.25×10^{-6} mol L^{-1}, **calculated from the 11 repeated measurements at the concentration of MLX of 5.0×10^{-6} mol L^{-1}.

Table 2 Comparison of the obtained results with those published in literature

Method	Electrode	Electrolyte	LOD [mol L^{-1}]	Real sample	Ref.
SSOP	DME	AcB (pH 4.76)	$3.0\times10^{-8*}$	tablets	29
DPP	DME	AcB (pH 4.88)	$5.7\times10^{-8*}$	spiked plasma	30
CAS SWV	HMDE	AcB (pH 5.0)	$2.0\times10^{-11*}$	spiked plasma	31
CAS DPV	HMDE	BRB (pH 4.0)	$2.9\times10^{-9**}$	tablets	32
LSV	CPE	BRB (pH 3.0)	$1.6\times10^{-7*}$	tablets	33
ASV	cysteic acid/GCE	BRB (pH 1.86)	$1.9\times10^{-9*}$	tablets spiked plasma	34
DPV	PLL/GO-COOH/GCE	BRB (pH 3.0)	$8.7\times10^{-7***}$	tablets spiked serum	35
AAS DPV	MIP@MWCNT/CPE	PB (pH 9.0)	$9.2\times10^{-11**}$	spiked plasma	36
ASV	GR/CPE	BRB (pH 2)	$2.6\times10^{-9***}$	tablets	37
DPV	BDDE	BRB (pH 3)	$5.9\times10^{-8**}$	tablets	Pres.

AAS DPV – anodic adsorptive stripping differential pulse voltammetry, AcB – acetate buffer solution, ASV – adsorptive stripping voltammetry, BRB – Britton-Robinson buffer solution, CAS SWV – cathodic adsorptive stripping square wave voltammetry, CAS DPV – cathodic

adsorptive stripping differential pulse voltammetry, CPE – carbon paste electrode, cysteic acid/GCE – cysteic acid modified glassy carbon electrode, DME – dropping mercury electrode, DPP – differential pulse polarography, DPV – differential pulse voltammetry GR/CPE – graphene nanoparticles modified carbon paste electrode, HMDE – hanging mercury drop electrode, LSV – linear-scan voltammetry, MIP@MWCNT/CPE – carbon paste electrode modified by molecularly imprinted polymer nanoparticle-multiwall carbon nanotubes, PB – phosphate buffer solution, PLL/GO-COOH/GCE – poly-L-lysine/carboxylated graphene oxide modified glassy carbon electrode, SSOP – single sweep oscillopolarography

[*]calculated as a signal to noise ratio of 3, [**]calculated as 3× standard deviation of an intercept divided by a slope, [***]calculation procedure was not specified

Verification of the proposed method was realized by determining a known amount of an analyte in model solutions. Concentration of MLX in a polarographic vessel was 1.0×10^{-6} mol L^{-1} in 15 mL of BRB (pH 3) and standard addition method was applied. Always 2-3 standard additions of standard solution of MLX (V = 15 μL, c_{MLX} = 0.001 mol L^{-1}) were added. Analysis was 5× repeated and parameters like average value with confidence interval, recovery and *RSD* of repeated determination were calculated. The obtained results summarized in Table 3 suggest that DPV with BDDE allows accurate, correct, and repeatable results (RSD_5 = 2.11 %).

3.3.3. Analysis of pharmaceutical samples

Finally, the developed method for voltammetric determination of MLX using BDDE was applied in the analysis of the pharmaceutical preparation, namely drug in tablet form Meloxicam Mylan with the declared MLX content of 15 mg per tablet. The procedure of sample preparation and analysis by standard addition method is described in detail in the experimental part. The analysis was 5× repeated again and one example of the obtained voltammograms together with the graphical evaluation of standard addition method is shown in Fig 7. The appropriated statistical parameters as in case of model solutions are placed in Table 3. It can be concluded that the obtained average value (15.25±0.27) corresponds with

that declared by producer and the determination of MLX in complicate matrix is also very well repeatable (RSD_5 = 2.33).

Table 3 Repeated determination of MLX in model solutions and pharmaceutical preparation

	Added [mol L^{-1}]	Found [mol L^{-1}]	Recovery [%]	RSD_5 [%]
model solution	1.0×10^{-6}	$(0.981\pm0.014)\times10^{-6}$	97.2-101.1	2.11
	Declared [mg/Tbl]	Found [mg/Tbl]	Recovery [%]	RSD_5 [%]
Meloxicam Mylan	15	(15.25±0.27)	98.1-103.6	2.33

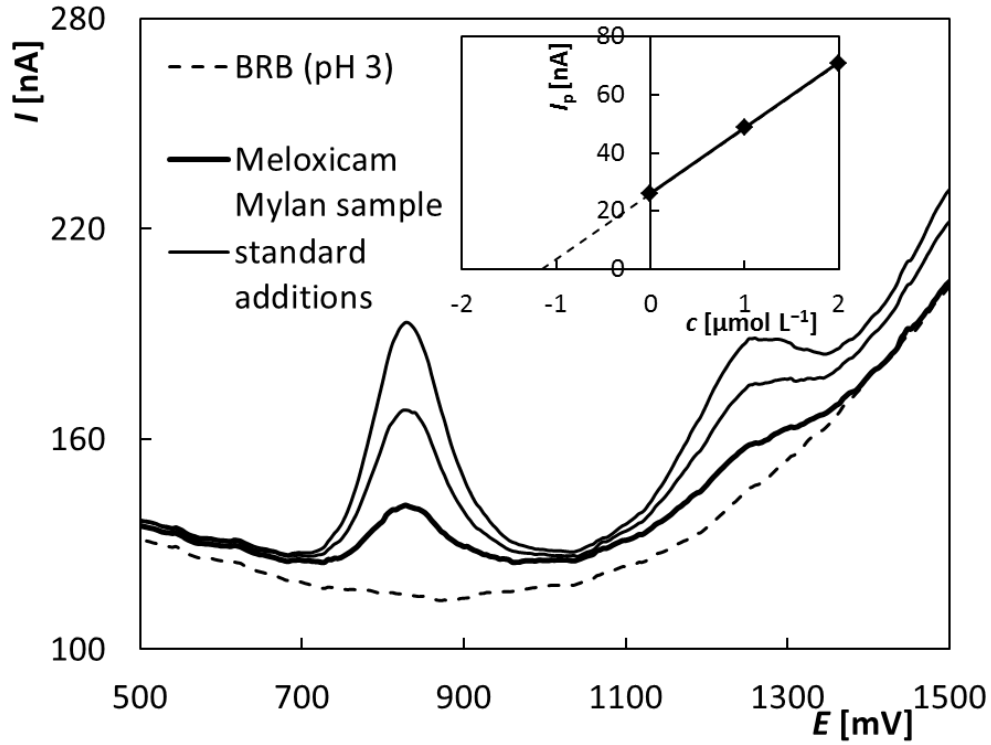

Figure 7 DPV voltammograms of analysis of pharmaceutical preparation "Meloxicam Mylan 15 mg" obtained on BDDE using standard addition method; supporting electrolyte – BRB (pH 3), E_{in} = 0 mV, E_{fin} = +2000 mV, v = 40 mV s^{-1}, pulse height = +60 mV, pulse width = 30 ms, standard additions – V = 15 µL, c_{MLX} = 0.001 mol L^{-1}; ***Inset:*** Graphical evaluation of standard addition method.

4 Conclusion

The electrochemical oxidation of a nonsteroidal anti-inflammatory drug meloxicam on BDDE proceeds in two irreversible voltammetric steps in wide pH range. Mechanism of the electrochemical oxidation was proposed and confirmed using high performance liquid chromatography/mass spectrometry analysis of MLX solutions electrolyzed on a carbon fiber brush electrode. Thiazole and benzoisothiazole were proved as the main reaction products of the first two-electron oxidation step. The second two-electron step includes probably subsequent oxidation of aldehyde group of thiazole to give the corresponding monoamide of oxalic acid.

Voltammetric method for MLX determination utilizing DPV in connection with BDDE was developed. The first anodic signal in BRB of pH 3 was found as optimum for analytical purposes and the basic parameters of DPV like scan rate, pulse height, and pulse width were optimized. The suitable BDDE pretreatment procedure was also suggested. The proposed method provides a wide *LDR* (2.5×10^{-7}-8.5×10^{-5} mol L^{-1}) and very low *LOD* (5.9×10^{-8} mol L^{-1}), which is significantly lower than that achieved for bulk CPE and comparable with those reported for various modified electrodes. Using model solutions, recovery of this method was ranging from 97.2-101.1 %. The applicability of the proposed method for practical samples was verified by successful analysis of pharmaceutical samples.

Acknowledgements This work was supported by the grant project of The Czech Science Foundation (project No. 17-03868S) and by The University of Pardubice (projects No. SGSFChT_2019_001).

References

[1] K. T. Olkkola, A. V. Brunetto, M. J. Mattila: Pharmacokinetics of oxicam nonsteroidal anti-inflammatory agents. Clin. Pharmacikinet. 26 (1994) 107-120.

[2] A. Barner: Review of clinical trials and benefit/risk ratio of meloxicam. Scand. J. Rheumatol. 25 (1996) 29-37.

[3] R. Fleischmann, I. Iqbal, G. Slobodin: Meloxicam. Expert Opin. Pharmacother. 3 (2002) 1501-1512.

[4] M. Ahmed, D. Khanna, D. E. Furst: Meloxicam in rheumatoid arthritis. Expert Opin. Drug Metab. Toxicol. 1 (2005) 739-751.

[5] C. J. Hawkey, J. Dequeker: Low gastrointestinal toxicity of meloxicam, a preferential inhibitor of the inducible cyclooxygenase (COX-2) enzyme compared to piroxicam. GUT 41 (1997) A7-A8.

[6] P. Staerkel, Y. Horsmans: Meloxicam-induced liver toxicity. Acta Gastro-Enterol. Belg. 62 (1999) 255-256.

[7] B. T. Villalba, F. R. Ianiski, A. G. Vogt, M. P. Pinz, A. S. Reis, R. A. Vaucher, M. P. Soares, E. A. Wilhelm, C. Luchese: Polymeric nanocapsules as a technological alternative to reduce the toxicity caused by meloxicam in mice. Regul. Toxicol. Pharmacol. 81 (2016) 316-321.

[8] E. Hoffman, D. M. Mladsi, B. Cryer, W. Hopkins, D. C. Brater, R. Parikh, R. Goyal, J. Castellsague, D. Stafkey-Mailey, C. Young: Dose-related risks of cardiovascular, gastrointestinal, and renal adverse events associated with meloxicam among patients with osteoarthritis: An observational study using US claims data. Arthritis Rheumatol. 68 (2016) 2359.

[9] K. Nakagawa, Y. Miyagawa, N. Takemura, H. Hirose: Influence of preemptive analgesia with meloxicam before resection of the unilateral mammary gland on postoperative cardiovascular parameters in dogs. J. Vet. Med. Sci. 69 (2007) 939-944.

[10] W. F. Huang, F. Y. Hsiao, Y. W. Tsai, Y. W. Wen, Y. T. Shih: Cardiovascular events associated with long-term use of celecoxib, rofecoxib and meloxicam in Taiwan - An observational study. Drug Saf. 29 (2006) 261-272.

[11] A. Mandi, M. Ahmad, M. Usman: New high performance liquid chromatographic method for simultaneous determination of diclofenac and meloxicam in oral formulation of liposomes and human plasma. J. Chem. Soc. Pak. 32 (2010) 654-661.

[12] A. Medvedovici, F. Albu, C. Georgita, C. Mircioiu, V. David: A non-extracting procedure for the determination of meloxicam in plasma samples by HPLC-diode array detection. Arzneimittelforschung-Drug Res. 55 (2005) 326-331.

[13] L. Leal, D. Bedor, E. Melo: Determination of meloxicam in human plasma administrated with four drugs by LC method: Application to a pilot bioavailability study. Lat. Am. J. Pharm. 30 (2011) 1883-1888.

[14] S. Cox, J. Bailey, M. White, K. Gordon, M. Souza: Determination of meloxicam in egg whites and yolks using reverse phase chromatography. J. Chromatogr. Sci. 55 (2017) 610-616.

[15] K. B. Liew, G. O. K. Loh, Y. T. F. Tan, K. K. Peh: Improved protein deproteinization method for the determination of meloxicam in human plasma and application in pharmacokinetic study. Biomed. Chromatogr. 28 (2014) 1782-1788.

[16] S. E. Vignaduzzo, P. M. Castellano, T. S. Kaufman: Method development and validation for the simultaneous determination of meloxicam and pridinol mesylate using RP-HPLC and its application in drug formulations. J. Pharm. Biomed. Anal. 46 (2008) 219-225.

[17] H. W. Lee, H. Y. JI, H. Y. KIM: Liquid chromatography-tandem mass spectrometry method for the determination of meloxicam and its metabolite 5-carboxymeloxicam in human plasma. Bioanal. 1 (2009) 63-70.

[18] Y. Z. Tian, X. Wu, M. J. Zhang, L. S. Zhao, Z. L. Xiong, F. Qin: Quantitative determination of meloxicam in dog plasma by high performance liquid chromatography-tandem mass spectrometry and its application in a pharmacokinetic study. Biomed. Chromatogr. 32 (2018) e4228.

[19] H. W. Lee, H. Y. Ji, H. Y. Kim, K. C. Lee, H. S. Lee: Liquid chromatography-tandem mass spectrometry method for the determination of meloxicam and its metabolite 5-carboxymeloxicam in human plasma. Bioanal. 1 (2009) 63-70.

[20] H. M. Rigato, G. D. Mendes, N. C. D. Borges, R. A. Moreno: Meloxicam determination in human plasma by high-performance liquid chromatography coupled with tandem mass spectrometry (LC-MS-MS) in Brazilian bioequivalence studies. Int. J. Clin. Pharmacol. Ther. 44 (2006) 489-498.

[21] M. Starek, J. Krzek: TLC determination of meloxicam in tablets and after acidic and alkaline hydrolysis. Acta Pol. Pharm. 69 (2012) 225-235.

[22] M. Mandrescu, A. F. Spac, V. Domeanu: Spectrophotometric determination of meloxicam. Rev. Chim. 60 (2009) 160-163.

[23] B. Gurupadaya, M. Trinath, K. Shilpa: Spectrophotometric determination of meloxicam by sodium nitroprusside and 1,10-phenanthroline reagents in bulk and its pharmaceutical formulation. Indian J. Chem. Technol. 20 (2013) 111-115.

[24] R. Rahmati, Z. Rafiee: A biocompatible high surface area ZnO-based molecularly imprinted polymer for the determination of meloxicam in water media and plasma. New J. Chem. 43 (2019) 8492-8501.

[25] V. Vasiliki, P. C. A. G. Pinto, M. L. M. F. S. Saraiva, J. L. F. C. Lima: Sequential injection determination of meloxicam in pharmaceutical formulations with spectrophotometric detection. Can. J. Anal. Sci. Spectrosc. 52 (2007) 351-358.

[26] E. M. Hassan: Spectrophotometric and fluorimetric methods for the determination of meloxicam in dosage forms. J. Pharm. Biomed. Anal. 27 (2002) 771-777.

[27] J. Tian, Ch. Li, L. Shaopu: A rapid and highly sensitive fluorimetric method for the determination of meloxicam using uranyl acetate, Anal. Methods. 6 (2014) 5221-5226.

[28] H. Y. Liu, L. Zhang, Y. H. Hao, Q. J. Wang, P. G. He, Y. Z. Fang: Flow-injection chemiluminescence determination of meloxicam by oxidation with N-bromosuccinimide. Anal. Chim. Acta 541 (2005) 187-192.

[29] H. Huang, H. Y. Gao, Y. H. Zeng: Single sweep oscillopolarography of meloxicam. Chin. J. Anal. Chem. 28 (2000) 1501-1503.

[30] S. Altinoz, E. Nemutlu, S. Kir: Polarographic behaviour of meloxicam and its determination in tablet preparations and spiked plasma. Farmaco 57 (2002) 463-468.

[31] A. E. Radi, M. Ghoneim, A. Beltagi: Cathodic adsorptive stripping square-wave voltammetry of the anti-inflammatory drug meloxicam. Chem. Pharm. Bull. 49 (2001) 1257-1260.

[32] A. M. Beltagi, M. M. Ghoneim, MM; A. Radi: Electrochemical reduction of meloxicam at mercury electrode and its determination in tablets. J. Phar. Biomed. Anal. 27 (2002) 795-801.

[33] A. Radi, M. A. El Ries, F. El-Anwar, Z. El-Sherif: Electrochemical oxidation of meloxicam and its determination in tablet dosage form. Anal. Lett. 34 (2001) 739-748.

[34] C. Y. Wang, Z. X. Wang, J. Guan, X. Y. Hu: Voltammetric determination of meloxicam in pharmaceutical formulation and human serum at glassy carbon electrode modified by cysteic acid formed by electrochemical oxidation of L-cysteine. Sensors 6 (2006) 1139-1152.

[35] S. Cheemalapati, B. Devadas, S. M. Chen: Novel poly-L-lysine/carboxyl-group enriched graphene oxide/modified electrode preparation, characterization and

applications for the electrochemical determination of meloxicam in pharmaceutical tablets and blood serum. Anal. Meth. 6 (2014) 8426-8434.

[36] S. Azodi-Deilami, E. Asadi, M. Abdouss, F. Ahmadi, A. H. Najafabadi, S. Farzaneh: Determination of meloxicam in plasma samples using a highly selective and sensitive voltammetric sensor based on carbon paste electrodes modified by molecularly imprinted polymer nanoparticle-multiwall carbon nanotubes. Anal. Meth. 7 (2015) 1280-1292.

[37] M. E. Eroglu, D. E. Bayraktepe, K. Polat, Z. Yazan: Electro-oxidation mechanism of meloxicam and electrochemical sensing platform based on graphene nanoparticles for its sensing pharmaceutical sample. Curr. Pharm. Anal. 15 (2019) 346-354.

[38] M. Iwaki, S. Sato, K. Takahashi, H. Sakairi: Electrical conductivity of nitrogen and argon implanted diamond. Nucl. Instr. Meth. 209 (1983) 1129-1133.

[39] Y. V. Pleskov, A. Y. Sakharova, M. D. Krotova, L. L. Bouilov, B. V. Spitsyn: Photoelectrochemical properties of semiconductor diamond. J. Electroanal. Chem. Interfac. Electrochem. 228 (1987) 19-27.

[40] K. Patel, K. Hashimoto, A. Fujishima: Application of boron-doped CVD-diamond film to photoelectrode. Denki Kagaku 60 (1992) 659-661.

[41] K. Patel, K. Hashimoto, A. Fujishima: Photoelectrochemical investigations on boron-doped chemically vapor-deposited diamond electrodes. J. Photochem. Photobiol. A: Chem. 65 (1992) 419-429.

[42] G. M. Swain, R. Ramesham: The electrochemical aktivity of boron-doped polycrystalline diamond thin film electrodes Anal. Chem. 65 (1993) 345-351.

[43] J. Xu, M. C. Granger, Q. Chen, J. W. Strojek, T. E. Lister, G. M. Swain: Boron-doped diamond thin-film electrodes. Anal. Chem. New Feat. 1 (1997) 591-597.

[44] R. G. Compton, J. S. Foord, F. Marken: Electroanalysis at diamond-like and doped-diamond electrodes. Electroanal. 15 (2003) 1349-1363.

[45] K. Peckova, J. Musilova, J. Barek: Boron-doped diamond film electrodes-New tool for voltammetric determination of organic compounds. Crit. Rev. Anal. Chem. 39 (2009) 148-172.

[46] J. H. T. Luong, K. B. Male, J. D. Glennon: Boron-doped diamond electrode: synthesis, characterization, functionalization, and analytical application. Analyst 134 (2009) 1965-1979.

[47] R. Selesovska, M. Stepankova, L. Janikova, K. Novaková, M. Vojs, M. Marton, M. Behul: Surface and electrochemical characterization of boron-doped diamond electrodes prepared under different conditions. Monatsh. Chem. 147 (2016) 1353-1364.

[48] K. Schwarzova-Peckova, J. Vosáhlova, J. Barek, I. Sloufova, E. Pavlova, V. Petrak, J. Zavazalova: Influence of boron content on the morphological, spectral, and electroanalytical characteristics of anodically oxidized boron-doped diamond electrodes. Electrochim. Acta 243 (2017) 170-182.

[49] R. Selesovska, B. Krankova, M. Stepankova, P. Martinkova, L. Janikova, J. Chylkova, M. Vojs: Influence of boron content on electrochemical properties of boron-doped diamond electrodes and their utilization for leucovorin determination. J. Electroanal. Chem. 821 (2018) 2-9.

[50] J. M. Freitas, T. D. Oliveira, R. A. A. Munoz, E. M. Richter: Boron-doped diamond electrodes in flow-based systems. Front. Chem. 7 (2019) No. 190.

[51] N. J. Yang, S. Y. Yu, J. V. Macpherson, Y. Einaga, H. Y. Zhao, G. H. Zhao, G. Swain, X. Jiang: Conductive diamond: synthesis, properties, and alectroanalytical applications. Chem. Soc. Rev. 48 (2019) 157-204.

[52] S. Baluchová, A. Daňhel, H. Dejmková, V. Ostatná, M. Fojta, K. Schwarzová-Pecková: Recent progress in the applications of boron doped diamond electrodes in electroanalysis of organic compounds and biomoleculs – A review. Anal. Chim. Acta 1077 (2019) 30-66.

[53] R. Selesovska, L. Janikova-Bandzuchova, J. Chylkova: Sensitive voltammetric sensor based on boron-doped diamond electrode for determination of the chemotherapeutic drug methotrexate in pharmaceutical and biological samples. Electroanalysis 27 (2015) 42-51.

[54] D. M. Stankovic, K. Katcher: The immunosuppressive drug - rapamycin - electroanalytical sensing using boron-doped diamond electrode. Electrochim. Acta 168 (2015) 76-81.

[55] M. Brycht, K. Kaczmarska, B. Uslu, S. A. Ozkan, S. Skrzypek: Sensitive determination of anticancer drug imatinib in spiked human urine samples by differential pulse voltammetry on anodically pretreated boron-doped diamond electrode. Diam. Rel. Mat. 68 (2016) 13-22.

[56] L. Svorc, K. Borovska, K. Cinkova, D. M. Stankovic, A. Plankova: Advanced electrochemical platform for determination of cytostatic drug flutamide in various matrices using a boron-doped diamond electrode. Electrochim. Acta 251 (2017) 621-630.

[57] R. Selesovska, B. Krankova, M. Stepankova, P. Martinkova, L. Janikova, J. Chylkova, T. Navratil: Voltammetric determination of leucovorin in pharmaceutical preparations using a boron-doped diamond electrode. Monatsh. Chem. 149 (2018) 1701-1708.

[58] M. Stepankova, R. Selesovska, L. Janikova, P. Martinkova, M. Marton, P. Michniak, J. Chylkova: Comparison of application options of boron-doped diamond electrodes with

various boron content for the determination of bioactive organic compounds. Chem. Listy 112 (2018) 389-395.

[59] S. Seyidahmet, F. Donmez, Y. Yardim, Z. Senturk: Simple, rapid, and sensitive electrochemical determination of antithyroid drug methimazole using a boron-doped diamond electrode. J. Iran. Chem. Soc. 16 (2019) 913-920.

[60] J. Skopalova, P. Bartak, P. Bednar, H. Tomkova, T. Ingr, I. Lorencova, P. Kucerova, R. Papousek, L. Borovcova, K. Lemr: Carbon fiber brush electrode as a novel substrate for atmospheric solids analysis probe (ASAP) mass spectrometry: Electrochemical oxidation of brominated phenols. Anal. Chim. Acta 999 (2018) 60-68.

[61] R. Jerga, V. Müllerová, J. Štěpánková, P. Barták, H. Tomková, J. Rozsypal, J. Skopalová: Phospholipid‐modified carbon fiber brush electrode for the detection of dopamine and 3,4‐dihydroxyphenylacetic acid. Monatsh. Chem. 150 (2019) 395-400.

[62] B. Bozal, B. Uslu: Applications of carbon based electrodes for voltammetric determination of lornoxicam in pharmaceutical dosage form and human serum. Comb. Chem. High T. Scr. 13 (2010) 599-609.

[63] A. A. J. Torriero, C. E. Tonn, L. Sereno, J. Raba: Electrooxidation mechanism of non-steroidal anti-inflammatory drug piroxicam at glassy carbon electrode. J. Electroanal. Chem. 588 (2006) 218-225.

[64] P. Luger, K. Daneck, W. Engel, G. Trummlitz, K. Wagner: Structure and physicochemical properties of meloxicam, a new NSAID. Eur. J. Pharm. Sci. 4 (1996) 175-187.

[65] S. Treimer, A. Tang, D. C. Johnson: A Consideration of the application of Koutecky-Levich plots in the diagnoses of charge-transfer mechanisms at rotated disk electrodes. Electroanalysis 14 (2002) 165-171.

[66] C. R. Wilke, P. Chang: Correlation of diffusion coefficients in dilute solutions. AIChE J. 1 (1955) 264-270.

[67] G. P. Cunningham, G. A. Vidulich, R. L. Kay: Several properties of acetonitrile-water, acetonitrile-methanol, and ethylene carbonate-water system: J. Chem. Eng. Data 12 (1967) 336-337.

[68] P. Kucerova, J. Skopalova, L. Kucera, J. Hrbac, K. Lemr: Electrochemical oxidation of fesoterodine and identification of its oxidation products using liquid chromatography and mass spectrometry. Electrochim. Acta 159 (2015) 131–139.

[69] A. T. Åberg, C. Olsson, U. Bondesson, M. Hedeland, A mass spectrometric study on meloxicam metabolism in horses and the fungus *Cunninghamella elegans*, and the relevance of this microbial system as a model of drug metabolism in the horse. J. Mass Spectrom. 44 (2009) 1026-1037.

[70] C. S. H. Jesus, V. C. Diculescu: Redox mechanism, spectrophotometrical characterisation and voltammetric determination in serum samples of kinases inhibitor and anticancer drug dasatinib. J. Electroanal. Chem. 752 (2015) 47-53.

[71] J. V. Macpherson: A practical guide to using boron doped diamond in electrochemical research. Phys. Chem. Chem. Phys. 17 (2015) 2935-2949.

Electrochemical oxidation of anti-inflammatory drug meloxicam and its determination using boron doped diamond electrode

Renáta Šelešovská,[a*] Frederika Hlobeňová,[a] Jana Skopalová,[b] Petr Cankař,[c] Lenka Janíková,[a] Jaromíra Chýlková,[a]

[a] *University of Pardubice, Faculty of Chemical Technology, Institute of Environmental and Chemical Engineering, Studentská 573, 532 10 Pardubice, Czech Republic*

[b] *Department of Analytical Chemistry, Faculty of Science, Palacký University in Olomouc, 17. listopadu 12, 771 46 Olomouc, Czech Republic*

[c] *Department of Organic Chemistry, Faculty of Science, Palacký University in Olomouc, 17. listopadu 12, 771 46 Olomouc, Czech Republic*

** e-mail: renata.selesovska@upce.cz*

Abstract

Voltammetric behavior of a nonsteroidal anti-inflammatory drug meloxicam was firstly studied using boron doped diamond electrode (BDDE). Two irreversible anodic current peaks were observed in wide pH range at potentials +900 mV and + 1400 mV vs. saturated silver-silver chloride electrode. Mechanism of the electrochemical oxidation was proposed and confirmed using high performance liquid chromatography/mass spectrometry analysis of electrolyzed meloxicam solutions. Subsequently, an analytical method for meloxicam determination was developed using differential pulse voltammetry in connection with BDDE. This method provides low limit of detection (5.9×10^{-8} mol L^{-1}) and wide linear dynamic range (2.5×10^{-7}-8.5×10^{-5} mol L^{-1}). Finally, model solutions as well as pharmaceutical preparations were successfully analyzed, and the meloxicam content was determined.

Key words

Meloxicam, Voltammetry, Oxidation, Boron-doped diamond electrode, Pharmaceutical samples

1 Introduction

Meloxicam (MLX, 4-hydroxy-2-methyl-*N*-(5-methyl-1,3-thiazol-2-yl)-2*H*-1,2-benzothiazine-3-carboxamide-1,1-dioxide, Scheme 1) is a nonsteroidal anti-inflammatory drug from the oxicam class (NSAID). Oxicams are a group of structurally closely related substances which are widely used in the treatment of both acute and chronic pain syndromes of various origins, especially vertebrogenic and joint pain. They are also applied for short-term treatment of postoperative and post-traumatic pain. In general, their analgesic, anti-inflammatory and antipyretic effects are used. They are also widely utilized in some types of headaches [1]. MLX is indicated especially for the treatment of rheumatoid arthritis, osteoarthritis and other joint diseases [2-4]. Due to its very low solubility in acidic environment, it can cause only few local gastrointestinal side effects [5-8]. MLX was also associated with an increased risk of serious cardiovascular adverse events [8-10].

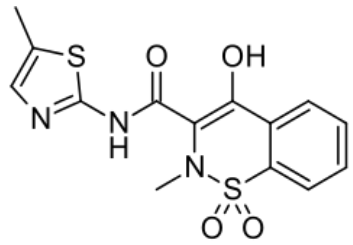

Scheme 1 Chemical structure of meloxicam.

MLX can be determined using various instrumental methods. High-performance liquid chromatography is most commonly used, *e.g.* in combination with diode or photodiode array detector [11, 12], UV spectrophotometric detector [13-16], or with mass spectrometer [17-20]. Method for separation and determination of MLX by thin-layer chromatography with densitometric detection was also described [21]. UV-VIS spectrophotometry [22-26] or fluorimetry [26, 27] represent another options for MLX determination. As an alternative, flow-injection chemiluminiscence determination can be also used [28]. These methods are

usually very sensitive and selective, but often require complex sample preparation for analysis and are time-consuming and instrumentally demanding. Because MLX is an electrochemically active compound, voltammetry offers a cheap, fast and simple alternative to the above mentioned methods.

In the first instance, reduction of MLX was utilized for its determination by single sweep oscillopolarography [29] and polarography [30] using dropping mercury electrode (DME). Hanging mercury drop electrode (HMDE) was used for MLX determination applying cathodic adsorptive stripping square wave voltammetry [31] as well as cathodic adsorptive striping differential pulse voltammetry [32]. The authors found that MLX provides two reduction signals on mercury electrode and Beltagi *et al.* [32] proposed the reduction mechanism of MLX. According to them, the first reduction step may be assigned to the reduction of the double bond in the enol form, while the second reduction step may correspond to the reduction of the carbonyl group of the keto form, to yield a saturated dihydrogen derivative. Radi *et al.* [33] studied the oxidative voltammetric behavior of meloxicam at a carbon paste electrode (CPE) and developed method for its determination using linear-scan voltammetry. According the authors, MLX gave rise to two voltammetric peaks, when the first one corresponds to the oxidation of amide functional group and the second one to the oxidation of enol functional group, respectively. Other published methods for MLX determination via its electrochemical oxidation used variously modified carbon based working electrodes. Wang *et al.* described method applying glassy carbon electrode (GCE) modified with anionic layer of cysteic acid providing electrostatic accumulation of the analyte onto the electrode surface [34]. MLX was also successfully determined at a poly-L-lysine (PLL)/carboxylated graphene oxide (GO–COOH)/modified glassy carbon electrode (GCE) [35], carbon paste electrode modified by molecularly imprinted polymer nanoparticle-multiwall carbon nanotubes [36], or graphene nanoparticles modified CPE [37]. A substantial

part of the last mentioned article is also devoted to the mechanism of MLX oxidation. In contrast to the mechanism reported in [33], the oxidation of the enol group is presumed to give rise to the first anodic signal and the oxidation of the amide group the second current response.

In the present work, MLX oxidation was firstly studied using boron doped diamond electrode (BDDE) [38-41]. This working electrode provide the number of advantages over traditionally employed electrodes, namely extreme hardness, high corrosion resistance, chemical inertness, high thermal conductivity, low sensitivity to dissolved oxygen, electrochemical stability in both alkaline and acidic media, very low and stable background current, and especially a wide usable potential window as well as a resistance to the electrode surface passivation [42-49]. These exceptional properties make it widely used in electroanalytical measurements in the determination of a number of biologically active substances and significant environmental contaminants as stated in various review articles [45, 50-52]. A number of studies related to drug determination were also described in the literature [53-59]. An oxidation mechanism of MLX was studied in more detail to clarify contradictory results reported in literature [33, 37]. The mechanism hitherto published was proposed based only on the results of pH effects on peak potential and peak current in cyclic voltammograms. Within our study, controlled potential electrolysis and ultraperformance liquid chromatography – mass spectrometry (UPLC/MS) with electrospray ionization (ESI) were used for generation and identification of products of MLX anodic oxidation. Finally, voltammetric method for MLX determination with BDDE was developed and utilized for analysis of a commercially available pharmaceutical preparation.

2 Experimental

2.1 Chemicals

Standard solution of 0.001 mol L^{-1} MLX (Sigma-Aldrich) was prepared by dissolution of the suitable amount in acetonitrile (Penta-Švec, Czech Republic). It was stored in a refrigerator at the temperature about +4°C and without light access. More dilute solutions were prepared fresh daily by dilution with supporting electrolyte. Britton-Robinson buffer (BRB) formed by acidic (0.4 mol L^{-1} H_3PO_4, H_3BO_3, and CH_3COOH, all from Penta-Švec, Czech Republic) and alkaline component (0.2 mol L^{-1} NaOH, Lachema, Czech Republic) was used as a supporting electrolyte. The solution of HNO_3 (pH 1) was diluted from 65 % HNO_3 (Penta-Švec, Czech Republic). The standard solutions of the other oxicams (Sigma-Aldrich), namely piroxicam (PRX), lornoxicam (LRX), and tenoxicam (TNX), were prepared by the same way as in case of MLX. Pharmaceutical preparation "Meloxicam Mylan 15 mg" originated from Generics (UK) Ltd, Great Britain.

2.2 Instrumentation

Voltammetric measurements were performed with Eco-Tribo Polarograph (Polaro-Sensors, Czech Republic) equipped with software POLAR.PRO version 5.1. The electrochemical cell was in a three-electrode arrangement. BDDE (Windsor Scientific, Great Britain, active surface area of 7.07 mm^2, inner diameter of 3 mm, resistivity of 0.075 Ω cm with a B/C ratio during deposition 1000 ppm) served as a working electrode, saturated argentchloride electrode (Ag/AgCl/KCl) was used as a reference and platinum wire as an auxiliary electrode (both Monokrystaly, Czech Republic). A potentiostat Autolab PGSTAT128 N (Metrohm Autolab, the Netherlands) was employed for linear sweep voltammetry (LSV) with rotating disc electrode (Autolab RDE, glassy carbon disc, diameter 0.5 cm) and controlled potential electrolysis with carbon fiber brush electrode (CFBE) [60]. Three-electrode system was completed with reference saturated calomel electrode (SCE) and platinum auxiliary electrode, which was placed in a cathodic compartment separated by a glass frit for bulk electrolysis.

Acquity UPLC system (Waters, USA) with PDA detector and mass spectrometric detector (QDA) equipped with heated electrospray ionization (HESI) and quadrupole analyzer were used for analysis of electrolyzed solutions. Potentiostat ADLC1 (Laboratorní přístroje, Czech Republic) with Model 5021A conditioning cell (ESA, Chelmsford, USA) containing porous graphite working electrode, Pd counter and a Pd/H_2 reference electrode, NE-1002X syringe pump (New Era Pump Systems, Farmingdale, USA) and Agilent 1100 Series LC/MSD Trap (Agilent Technologies, Palo Alto, USA) with electrospray ionization (ESI) were employed for on-line EC/MS experiments.

All measurements were carried out at laboratory temperature of 23±2 °C.

Values of pH were measured by pH-meter Accumet AB150 (Fisher Scientific, Czech Republic) and dissolution of standards as well as pharmaceutical samples was facilitated applying ultrasonic bath Bandelin Sonorex (Schalltec GmbH, Germany). Polishing kit (Electrochemical Detectors, Czech Republic) consisted of a polyurethane pad and Al_2O_3 powder (particle size 0.3 μm) was used for BDDE pretreatment.

Parameters of calibration curves and confidence intervals were calculated on the level of significance 0.05. Statistical parameters like limit of detection (LOD) and limit of quantification (LOQ) were calculated from the calibration dependences as 3× and 10×, respectively, of standard deviation of an intercept divided by a slope.

2.3 Procedures

2.3.1 Voltammetric measurements

Before beginning of the experiments, BDDE was activated and regenerated employing 20 cyclic voltammograms between initial potential (E_{in}) −1000 mV and switching potential (E_{switch}) +2200 mV directly in supporting electrolyte. Cycling was terminated at the positive potential values, *i.e.*, the final potential (E_{fin}) was +2200 mV. After this step, the working

electrode was ready for analysis. Between the particular measurements, no regeneration or activation step was inserted. This procedure ensured the O-terminated surface because BDD is easily oxidizable even by air oxygen.

Cyclic voltammetry (CV) was utilized for the investigation of the voltammetric behavior of MLX. If not defined otherwise, measurements were performed from E_{in} = −500 mV to E_{switch} = +2000 mV and back to −500 mV applying the scan rate (v) of 100 mV s^{-1}. In case of the scan rate study, the value of v varied from 25 to 500 mV s^{-1}. Considering very good sensitivity, differential pulse voltammetry (DPV) was used for the development of the method for MLX determination. BRB of pH 3 was chosen as a suitable supporting electrolyte. The optimized DPV parameters were as follows: E_{in} = 0 mV, E_{fin} = +2000 mV, v = 40 mV s^{-1}, pulse height +60 mV, and pulse width 20 ms (and another 20 ms as a current sampling time). The values of the peak height (I_p) were evaluated according to the baseline inserted as a tangent to the curve at minimum before and after the peak. Hydrodynamic voltammograms were recorded with RDE using LSV at scan rate 10 mV s^{-1} and rotation speed 500-3000 rpm (52–314 rad s^{-1}). Glassy carbon electrode disk was polished before each scan with alumina slurry (0.05 μm particle size) on microcloth (Buehler).

2.3.2. Controlled potential electrolysis, HPLC/MS analysis and EC/MS experiments

Carbon fiber brush electrode (CFBE) used as the working electrode for bulk electrolysis was prepared in the laboratory according to the previously described procedure [61]. Before use, CFBE was sonicated in acetonitrile and deionized water for 5 minutes. Subsequently, it was electrochemically pretreated in 0.1 mol L^{-1} H_2SO_4 using 50 potential cycles from -1.7 to +2.0 V (vs. SCE) and thoroughly washed with deionized water. Controlled potential electrolysis was performed with 4 mL of 5×10^{-4} mol L^{-1} MLX solution in the mixture of 0.2 mol L^{-1} aqueous CH_3COOH and CH_3CN (1/1, v/v) in anodic compartment of the electrolytic cell, at

potentials of 0.8 V and 1.2 V (vs. SCE) for 60 min on the electromagnetic stirrer. The cathodic compartment was filled with 0.2 mol L^{-1} CH_3COOH. Electrolyzed samples and respective standard solution of MLX were analyzed by UPLC/MS. Chromatographic separation was performed on XSelect HSS T3 column (3 mm × 50 mm, 2.5 μm, Waters) at 23 °C. Mobile phase consisted of 0.01M aqueous ammonium acetate (solvent A) and a mixture CH_3CN/H_2O (90/10, v/v, solvent B). Gradient elution: 0–5 min (0–55 % B), 5–10 min (55 % B) was performed with flow rate 0.6 mL min^{-1}. After the analysis the column was equilibrated with solvent A for 2.5 min. The injection volume was 5 μL. Mass spectrometry conditions were set for both positive (ESI+) and negative (ESI-) electrospray ionization modes as follows: capillary voltage 0.8 kV, cone 25 V, source temperature 120 °C, heated probe temperature 600 °C and the acquired mass range *m*/*z* 60–600.

In on-line EC/MS experiments, MLX solution (c = 5×10^{-5} mol L^{-1}) in 0.2 mol L^{-1} aqueous CH_3COOH and CH_3CN (1/1, v/v) was pumped through the coulometric cell to the electrospray ion source of MS by flow rate 8 μL min^{-1}. Potential of the working porous graphite electrode in the cell gradually increased from 0 to 0.7 V (vs. Pd/H_2) in steps of 20 mV. At each potential, MS signals were recorded for 60 s in both positive and negative ESI modes under the following conditions: drying gas (N_2), flow rate 5 L min^{-1}, drying temperature 180 °C, nebulizer pressure 15 psi, capillary voltage ±3.5 kV, end plate offset ±0.5 kV. Helium was used as collision gas. Data were processed using DataAnalysis 3.3 software (Bruker Daltonik, Germany).

2.3.3 Analysis of pharmaceutical sample

The stock solution for the quantitative experiments was prepared from one blister of MLX tablets of “Meloxicam Mylan 15 mg” containing 10 tablets with declared content of 15 mg MLX/Tbl. Tablets were powdered in a grinding mortar, and then the sample was

quantitatively transferred into a 1000 mL standard flask and was dissolved in acetonitrile applying the ultrasonic bath. This solution was filtered. The concentration of MLX in the prepared solution was about 4.27×10^{-4} mol L^{-1} (calculated according to the content of the substance declared by the producer). 35 µL of the sample solution was added to the polarographic cell with 15 mL of the supporting electrolyte (BRB pH 3) and the determination was carried out by the standard addition method and two standard additions (15 µL of 0.001 mol L^{-1} MLX) were applied at least. The determination was five times repeated and relative standard deviation of repeated determination (*RSD*) was calculated.

3 Results and discussion

3.1. Voltammetric behavior of meloxicam

Oxidation of MLX on BDDE was firstly measured in BRB (pH 3) at 100 mV s^{-1}. These conditions were taken from the literature [33]. The obtained cyclic voltammogram of 1.0×10^{-5} mol L^{-1} MLX is depicted in Fig. 1 (red curve). In accordance with the literature, MLX provided two oxidation signals at the potential values (E_p) of +900 and +1400 mV. No corresponding reduction peak was observed on the cathodic curve, suggesting an irreversible course of the ongoing electrode reaction. This finding was confirmed also during the measurements with different E_{switch} values as it is evident from the inset of Fig. 1.

According to the authors of the previous publication [33], the first MLX peak corresponds to the oxidation of amide function group and the second one to the oxidation of enol function. Eroglu *et al.* [37] assigned the first signal to the oxidation of enol group and the second one to the oxidation of amide. None of the research groups provided any evidence to support their proposal (*e.g.*, mass spectroscopy analysis of the products of electrolysis). Moreover, CV voltammograms of other oxicams (PRX, LRX, and TNX) were preliminary measured on the same BDDE and for comparison they are placed in Fig. 1 too. All these

compounds provide one oxidation signal at the same E_p as the first peak of MLX which predicts the same electrochemical process. In the literature [62, 63], this peaks are also assigned to the oxidation of enol group. In the following chapters we would like to clarify the oxidation mechanism of MLX among others using HPLC-MS technique.

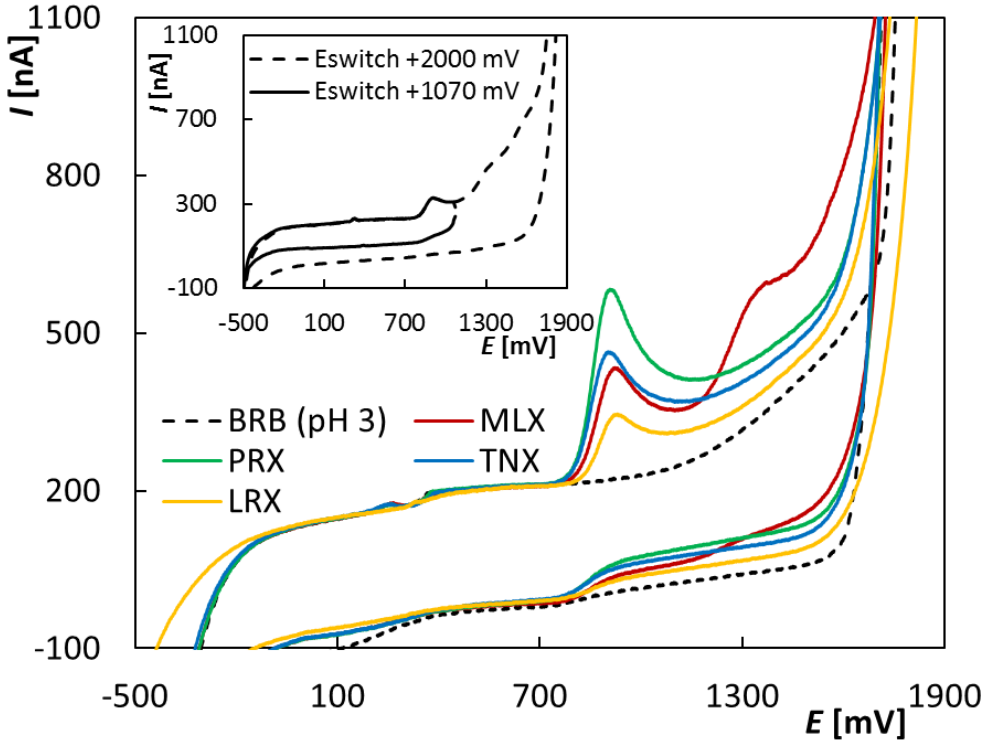

Figure 1 Cyclic voltammograms of oxicams in BRB (pH 3) obtained on BDDE; E_{in} = −500 mV, E_{switch} = +2000 mV, v = 100 mV s^{-1}, c_{MLX} = c_{PRX} = c_{LRX} = c_{TNX} = 1.0×10^{-5} mol L^{-1}; ***Inset:*** Cyclic voltammograms of MLX with E_{switch} = +2000 and +1070 mV.

3.1.1. Dependence on pH

Fig. 2 shows the influence of pH of supporting electrolyte in the range from 1 to 12 on MLX (1.0×10^{-5} mol L^{-1}) anodic signals obtained by CV (v = 100 mV s^{-1}). The acidic medium was ensured with the solution of diluted HNO_3, and other pH values (2-12) were reached using BRB. It is evident that the best developed two peaks were observed in acidic media (pH 1-3) and with the increasing of pH both signals decrease and widen. In alkaline electrolyte the first peak became very difficult evaluable and the second one disappeared. Due to the following

analytical usage, attention was paid especially to the first peak. Its position shifts to more negative potential values in the range of pH 1-3 and shows a shift in the opposite direction in more basic media (see the inset of Fig. 2). The peak height (I_p) reached maximum in acidic medium (pH 1-3) as it is documented in the inset of Fig. 2. Changes in trends of both I_p and E_p of the first MLX peak in the dependence on pH indicate the change in protolytic forms of MLX. As reported [64], MLX has two pK_a values: 1.09 and 4.18. At low pH values (<1.09), MLX exists mainly in the cation form, at pH > 4.18 the anion form prevail in aqueous solutions. The pH dependence of I_p and E_p shows that the anionic form of MLX is more difficult to oxidize than the protonated and uncharged form. BRB of pH 3 was applied as suitable supporting electrolyte for all next voltammetric measurements.

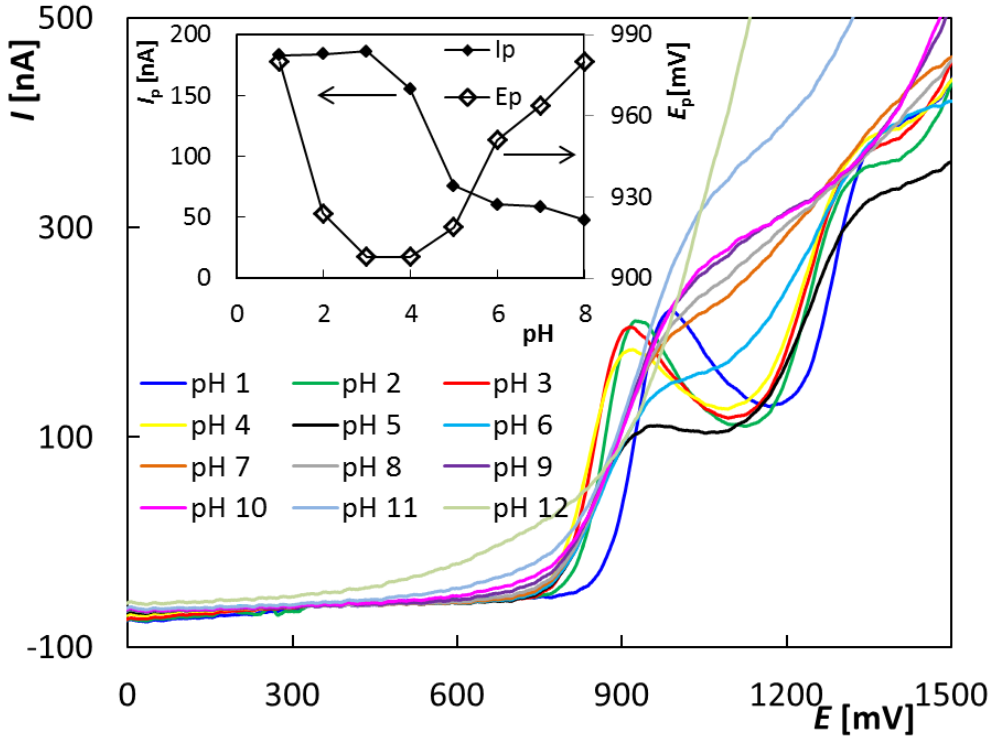

Figure 2 Anodic parts of cyclic voltammograms of MLX obtained on BDDE in dependence on pH; supporting electrolyte – solution of HNO_3 (pH 1) and BRB (pH 2-12), E_{in} = −500 mV, E_{switch} = +2000 mV, v = 100 mV s^{-1}, c_{MLX} = 1.0×10^{-5} mol L^{-1}; ***Inset:*** Dependence of I_p and E_p of the first oxidation peak on pH of supporting electrolyte.

3.1.2. Dependence on scan rate

The effect of scan rate on the voltammetric behavior of MLX can be useful for determining the controlling process and for proposing mechanism of the observed electrode reactions. CV voltammograms of MLX (1.0×10^{-5} mol L^{-1}) obtained in BRB (pH 3) on BDDE in dependence on v (50-450 mV s^{-1}) are shown in Fig. 3. It is evident that both anodic signals increased with growing v and simultaneously their E_p shifted to more positive potential values confirming the irreversible course of the oxidation reactions. While dependence of I_p on v for the first signal, that we are interested in (inset of Fig. 3), did not show a linear pattern, dependence of I_p on square root of v (I_p_$v^{1/2}$) was linear and can be described by equation (1) with the appropriate correlation coefficient. This indicates the diffusion-controlled process. It was verified also with logarithmic dependence (log(I_p)_log(v)) described by equation (2). The significant influence of kinetics was also proved because the value of slope lies below the theoretical value of 0.5.

$$I_p\ [\mathrm{nA}] = (38.5 \pm 2.1)\ (v\ [\mathrm{mV\ s^{-1}}])^{1/2} + (203 \pm 33),\ r = 0.9901 \quad (1)$$

$$\log\left(I_p\ [\mathrm{nA}]\right) = (0.368 \pm 0.011) \log\ (v\ [\mathrm{mV\ s^{-1}}]) + (2.030 \pm 0.028),\ r = 0.9963 \quad (2)$$

Consistent with the findings of the pH-dependency study, an increasing effect of kinetics with increasing pH was observed. While at pH 1 the slope of log(I_p)_log(v) (equation 3) is very close to the theoretical value of 0.5 for a pure diffusion-controlled process, at pH 5 (where the anionic form of MLX predominates) the slope value 0.31 (equation 4) is lower than at pH 3 (equation 2), showing that the influence of kinetics on the control process increases with pH.

$$\log\left(I_p\ [\mathrm{nA}]\right) = (0.4741 \pm 0.0088) \log\ (v\ [\mathrm{mV\ s^{-1}}]) + (1.425 \pm 0.020),\ r = 0.9991 \quad (3)$$

$$\log\left(I_p\ [\mathrm{nA}]\right) = (0.3110 \pm 0.0128) \log\ (v\ [\mathrm{mV\ s^{-1}}]) + (1.313 \pm 0.028),\ r = 0.9099 \quad (4)$$

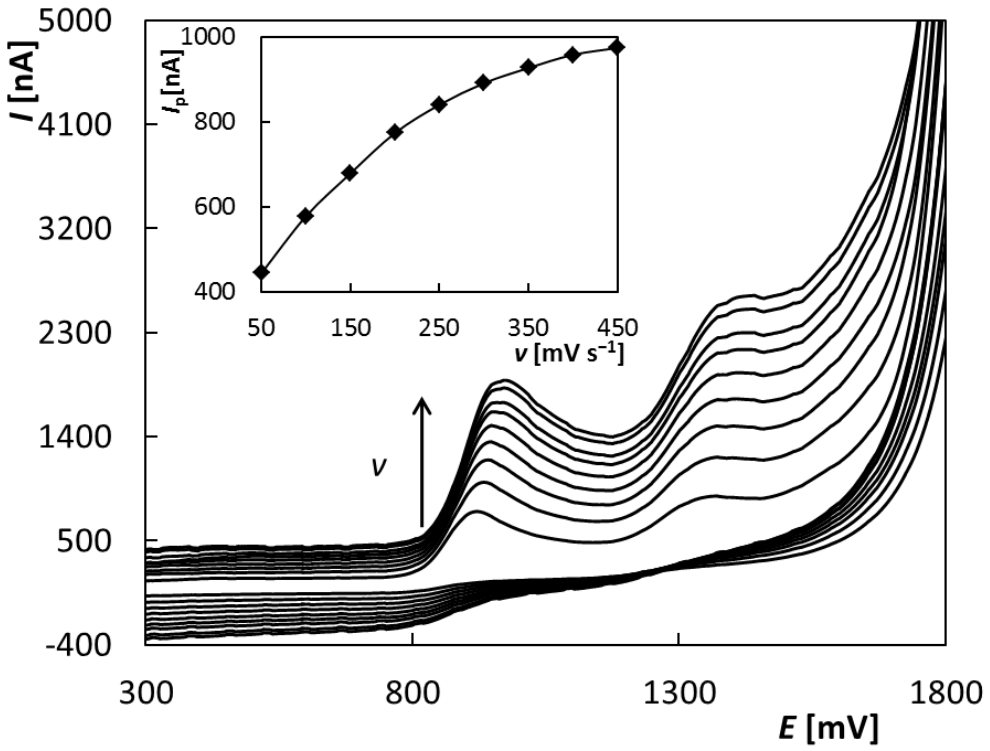

Figure 3 Cyclic voltammograms of MLX obtained on BDDE in dependence of scan rate; supporting electrolyte – BRB (pH 3), E_{in} = −500 mV, E_{switch} = +2000 mV, v = 50-450 mV s^{-1}, c_{MLX} = 1.0×10^{-5} mol L^{-1}; ***Inset:*** Dependence of I_p on pH of supporting electrolyte.

3.2. Oxidation mechanism

3.2.1. Number of exchanged electrons

Linear sweep voltammograms of MLX recorded on RDE at different rotation velocity were evaluated and used to estimate number of electrons transferred at anodic oxidation of MLX. As the electrochemical reaction evinced mixed diffusion-kinetic control, Koutecký-Levich equation (5) was used to calculate number of involved electrons from the slope of the dependence of $1/I$ on $1/\omega^{1/2}$ [65]:

$$\frac{1}{I} = \frac{1}{0.62nFAD_{\mathrm{A}}^{2/3}\upsilon^{-1/6}c_{\mathrm{A}}\omega^{1/2}} + \frac{1}{nFAk_h c_{\mathrm{A}}}, \quad (5)$$

where I represents electrode current, n is number of electrons, F is the Faraday constant, A is area of the disc electrode (0.196 cm^2), υ is the kinematic viscosity of the solution (8.84×10^{-3} cm^2 s^{-1}), c_A - concentration of analyte (9.52×10^{-8} mol cm^{-3}), ω – rotating velocity (rad s^{-1}) and k_h – heterogenous rate constant (cm s^{-1}). Diffusion coefficient D_A of MLX was estimated from the Wilke-Chang equation (6) [66]:

$$D_A = 7.4 \times 10^{-8} \frac{T(xM)^{0.5}}{\eta V^{0.6}}, \quad (6)$$

where T is thermodynamic temperature, η is viscosity, x and M are association parameter and molar weight of the solvent, respectively, and V is molar volume of the solute. Under the respective experimental conditions T = 298.15 K, viscosity of 1:1 (v/v) acetonitrile – water mixture η = 0.801 cP [67], x = 2.6, M = 18.015 g mol^{-1} and molar volume of MLX V = 217.7±3.0 mL (calculated using ACD/ChemSketch software), the value of D_A = 0.746×10^{-5} cm^2 s^{-1} was obtained. Slopes of the dependence $1/I = f(1/\omega^{1/2})$ were evaluated from hydrodynamic voltammograms of MLX (Fig. S1-A, B in Supplementary information file) at 5 different potentials (0.8-1.0 V) and each value was used to calculate number of electrons with the result: n = 2.09±0.11. This result corresponds to the number of electrons n = 1.98 found by convolutive procedure [68] applied to linear sweep voltammogram recorded on a static disc electrode (see Fig. 2 in Supplementary material). It can be concluded, that the first step of the anodic oxidation of meloxicam is a two-electron process.

3.2.2. UPLC/MS analysis of oxidation products

The previously proposed mechanisms of electrochemical oxidation of MLX in aqueous solutions attribute the first oxidation step to either the amide function group [33] or the enol group [37]. Both hypotheses are based on the results of the voltammetric behavior of this substance and its similarity to the behavior of structurally related substances. In this work, we

attempted to elucidate the reaction mechanism based on UPLC/MS analysis of MLX electrolysis products produced on large-area CFBE. For comparison, on-line EC/MS experiments were performed with flow-through coulometric cell containing working porous graphite anode coupled to mass spectrometer with ion trap analyzer. In both types of experiments, 0.2 mol L^{-1} aqueous CH_3COOH with acetonitrile (1/1, v/v) was used to provide the appropriate acidic medium and to maintain MLX in solution. Potentials for the bulk electrolysis in the off-line experiment were selected from hydrodynamic voltammograms (Fig. S1-A in the Supplementary information file) at the limiting current of the first anodic wave and at the steep part of the second waves (to avoid formation of hydrogen bubbles in the narrow cathodic compartment at higher potentials).

UPLC/MS analysis of the standard MLX solution provided a single peak with retention time t_r = 4.62 min and protonated molecule $[M+H]^+$ at *m*/*z* 352 (Fig. S3a and S4a in the Supplementary information file, respectively). Fragmentation pattern of the spectrum acquired in ESI+ mode (Fig. S4a) with fragment ions at *m*/*z* 115, 141 and 184 corresponds to those reported in the literature [69] Mass spectrum recorded in ESI- mode (Fig. S4b) shows fragments at *m*/*z* 286 (loss of SO_2), *m*/*z* 210 and *m*/*z* 146 (loss of SO_2 from the fragment *m*/*z* 210).

Total ion current chromatogram of the MLX solution electrolyzed at potential of +0.8 V, corresponding to the limiting current of the first voltammetric wave of MLX, revealed four main peaks of reaction products (Fig. S3b in Supplementary information file). Two peaks with t_r = 4.30 min and t_r = 5.83 min and *m*/*z* 350 appertain to isomeric products with the *m*/*z* value two units lower than that of MLX. Mass spectra of these products are similar (Fig. S5) with common fragment ions at *m*/*z* 210 and *m*/*z* 141, which differ in their intensities. Presence of the fragment *m*/*z* 141 corresponding to the methyl-thiazolyl carboxamide moiety, which is characteristic of MLX, confirms that this part of the molecule

remain unchanged. The third peak with t_r = 5.32 min belongs to a product with $[M+H]^+$ at *m*/*z* 368 (Fig. S6a in the Supplementary information file). The main fragment at *m*/*z* 141 indicates presence of unchanged methyl-thiazolyl carboxamide moiety of the product. The fourth peak with t_r = 3.52 min, $[M+H]^+$ at *m*/*z* 171 (Fig. S6b in the Supplementary information file) rendered fragment ions at *m*/*z* 143 and *m*/*z* 115 corresponding to two consecutive losses of CO from two carbonyl groups in the product structure. These results indicate that all products of the first step of meloxicam oxidation have an unchanged methyl-thiazolyl carboxamide structure. Therefore, in the first step of the electrochemical reaction, oxidation occurs at the enol group of the hydroxybenzothiazine ring.

Chromatogram of the MLX solution electrolyzed at potential of +1.2 V corresponding to the steep part of the second oxidation wave of MLX, gave a peak with retention time t_r = 3.18 min and *m*/*z* 187 in ESI+ or *m*/*z* 185 in ESI- (Fig. S7 in the Supplementary information file). Fragments at *m*/*z* 143 and 141 formed by losses of CO_2 and HCOOH, respectively, confirm that the product is a carboxylic acid having unchanged methyl-thiazolyl carboxamide moiety (**9** in Scheme 2).

The products detected in the electrolyzed MLX solutions by UPLC/MS were also observed in on-line EC/MS experiments that may detect unstable reaction products. MS signal intensity of individual reaction products varied with the potential applied to the working electrode in accordance with the UPLC/MS analysis of MLX solutions electrolyzed at lower and higher potential (Fig. S8 in the Supplementary information file). In addition, in the mass spectra obtained at higher potentials of electrolysis, one more product was observed at *m*/*z* 296 in ESI+. Collision spectrum of this product (Fig. S9, Supplementary information file) gave major fragments at *m*/*z* 253 (loss of NCOH), *m*/*z* 235 (subsequent loss of H_2O) and *m*/*z* 210, corresponding to unchanged *N*-methyl benzothiazinone moiety. This product was found in UPLC/MS analysis only at very low content, indicating its low long-term stability.

However, this finding shows that the amide or methylthiazole group of MLX can be subjected to an electrochemical reaction at sufficiently high potential.

3.2.3. Reaction mechanism

Voltammetric experiments revealed that the electrochemical oxidation of MLX proceeds in two irreversible steps, preferably under acidic conditions. Based on the identified products of electrolysis performed at the limiting current of the first two-electron wave, the following reaction mechanism was proposed (Scheme 2): The electrode reaction starts with the electron transfer from the hydroxyl oxygen of the enol group. Deprotonation of the formed cation radical and subsequent transfer of the second electron leads to intermediate **2**, which is susceptible to form **3** by addition of water and its ring-chain tautomeric form **4**. Formation of the structure **3** is consistent with reaction mechanism proposed for electrochemical oxidation of a relative drug piroxicam [63]. Under acidic conditions, intramolecular condensation of **4** leads to benzoisothiazoliminium form **5**, which can be hydroxylated to give unstable intermediate **6**. Decomposition of **6** produces thiazole (**7**) and benzoisothiazole (**8**), the two main reaction products of the first electrochemical oxidation step of MLX. As the first reaction step starts with the electron withdrawing from the "enolic" hydroxyl, after its deprotonation at pH > pK_a (4.18) the electrode reaction becomes kinetically controlled by the rate of protonation of the deprotonated enolate.

Second step of the electrochemical oxidation includes most likely subsequent oxidation of aldehyde group of **7** to give the corresponding monoamide of oxalic acid (**9**). However, oxidation of the methylthiazole moiety to corresponding sulfone and sulfoxide [70] can also be supposed according to the results of EC/MS experiment. Hydrolytic cleavage of the sulfoxide can lead to formation of the detected product at *m*/*z* 296 in ESI+.

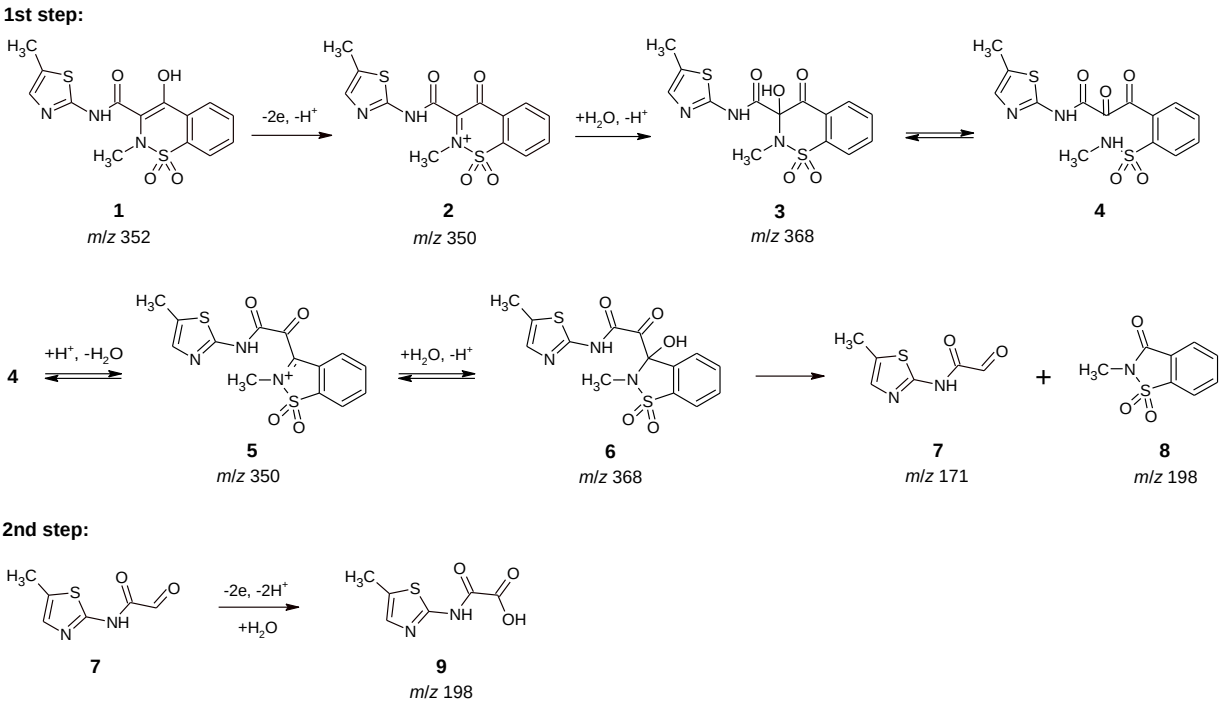

Scheme 2 Proposed mechanism of the first and second step of electrochemical reactions of meloxicam with mass-to-charge ratios in positive ion mode ESI-MS.

3.3. Voltammetric determination of meloxicam

3.3.1. Optimization of DPV parameters

DPV was applied for the development of voltammetric method for MLX determination and the first oxidation peak was used for this purpose. At the beginning, basic parameters of DPV like scan rate, pulse height and pulse width were optimized. All the following experiments were carried out in BRB of pH 3 and with the MLX concentration of 5.0×10^{-6} mol L^{-1} in a polarographic vessel. One parameter was always changed and the others were kept constant. Specific settings are described in the caption of the Fig. 4 which illustrates the courses of the particular dependences of I_p on the individual tested parameters. The value of v was changed from 10 to 100 mV s^{-1}. Fig. 4A shows the peak increased up to 40 mV s^{-1} and therefore this value was set for all the following measurements. The pulse height was tested in the range

from 10 to 100 mV. I_p increased approximately linearly in dependence of pulse height up to value 70 mV (Fig. 4B) but simultaneously at the higher values MLX oxidation signal was spreading. For further experiments, a pulse height of 60 mV was selected as a compromise between peak height and shape. The last examined parameter – pulse width was tested in the range of 10-100 ms (Fig. 4C) and the value of 30 ms was applied for all of the future experiments.

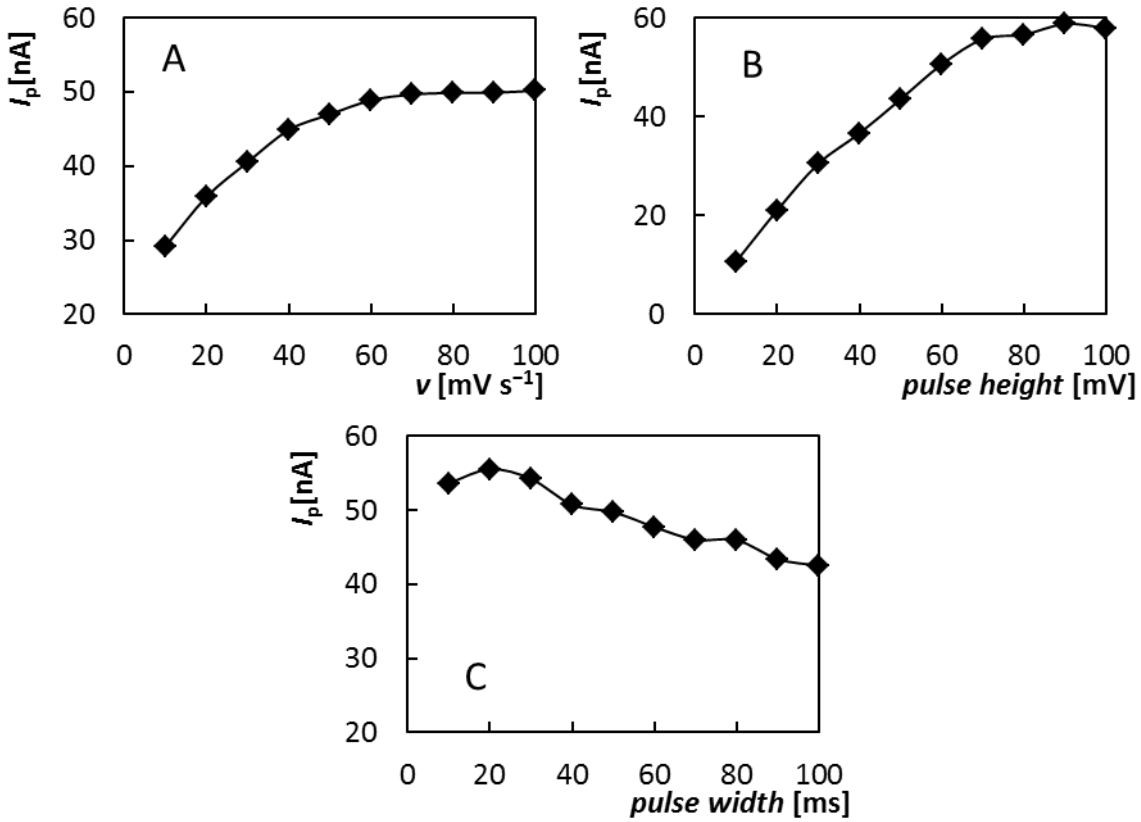

Figure 4 Dependences of I_p on v (A), I_p on pulse height (B), and I_p on pulse width (C) obtained on BDDE using DPV; supporting electrolyte – BRB (pH 3), E_{in} = 0 mV, E_{fin} = +2000 mV, v = 10-100 mV s^{-1} (A), and 40 mV s^{-1} (B, C), pulse height = +50 mV (A), +10-+100 mV (B), and +60 mV (C), pulse width = 50 ms (A, B), 10-100 ms (C), c_{MLX} = 5.0×10^{-6} mol L^{-1}.

Another factor, that significantly influences the electrochemical properties of BDDE surface and thus the height and shape of the measured current signals, is the pretreatment

procedure [71]. In case of MLX determination we tested four different pretreatment processes as follows: (i) anodic pretreatment (E = +2400 mV, t = 300 s), (ii) cathodic pretreatment (E = −2000 mV, t = 300 s), (iii) insertion of 20 cyclic voltammograms (E_{in} = −1000 mV, E_{switch} = E_{fin} = +2200 mV, v = 100 mV s^{-1}), and (iv) polishing on alumina. DPV voltammograms of MLX (5.0×10^{-6} mol L^{-1}) obtained under the optimized parameters always after the insertion of particular pretreatment procedure directly in analyzed solutions before scan are illustrated in Fig. 5. It is evident that the highest and the sharpest peaks were obtained similarly after cycling and anodic pretreatment that both provide O-terminated BDDE surface. On the other hand, the lowest signal was recorded after application of negative potential and reduction of the working surface, respectively (H-terminated surface). Concerning polishing, significant background increase and worsening of the repeatability of measurement was observed. Due to the better repeatability and slightly higher peak, CV was selected as suitable pretreatment procedure for all further measurements. Moreover, it was found that it is sufficient to include cycling only at the beginning of the work. There is no need to activate or regenerate the electrode surface between the individual measurements. The electrode passivation does not occur, which is confirmed by the obtained low value of relative standard deviation of 11 repeated measurements (RSD_{11} = 0.3 %) of 5.0×10^{-6} mol L^{-1} MLX.

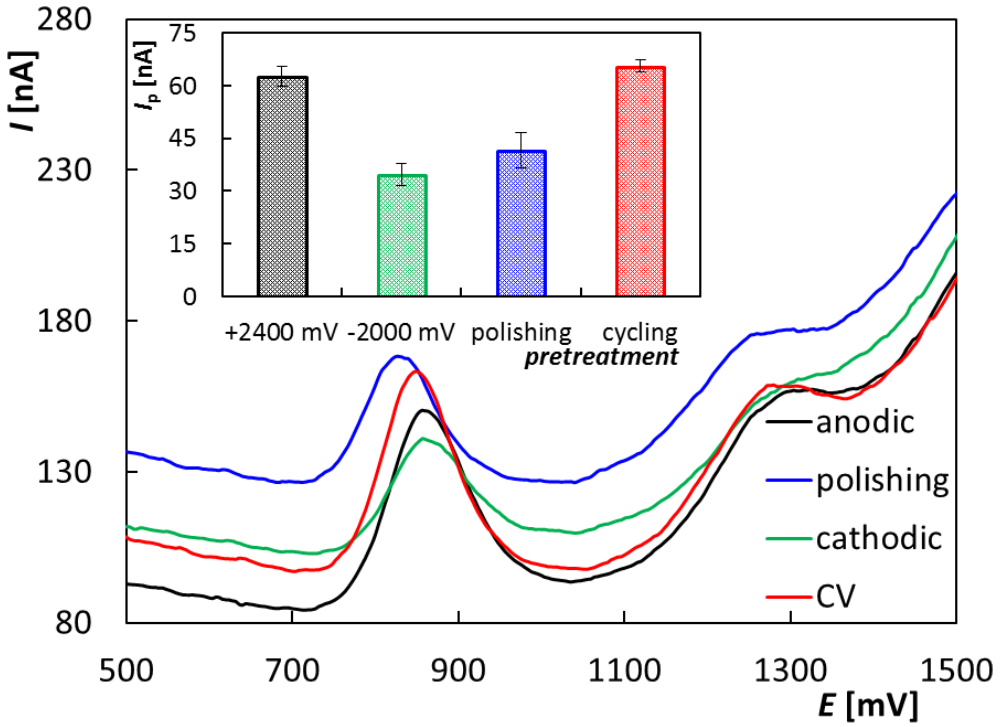

Figure 5 DPV voltammograms of 5×10^{-6} mol L^{-1} MLX obtained on BDDE after different pretreatment procedure; supporting electrolyte – BRB (pH 3), E_{in} = 0 mV, E_{fin} = +2000 mV, v = 40 mV s^{-1}, pulse height = +60 mV, pulse width = 30 ms, c_{MLX} = 5.0×10^{-6} mol L^{-1}; ***Inset:*** Dependence of I_p on applied pretreatment procedure: (i) anodic pretreatment – E = +2400 mV, t = 300 s, (ii) cathodic pretreatment – E = −1000 mV, t = 300 s, (iii) cycling – 20 cyclic voltammograms, E_{in} = −1000 mV, E_{switch} = E_{fin} = +2200 mV, v = 100 mV s^{-1}, (iv) polishing – in alumina.

3.3.2. Analysis of model solutions

New voltammetric method was applied to measurement of various concentration dependences of MLX in model solutions to determine the basic statistical parameters like linear dynamic range (*LDR*), *LOD*, and *LOQ*. In Fig. 6, an example of the recorded DPV voltammograms in dependence on MLX concentration in the range from 1.0×10^{-6} to 1.7×10^{-5} mol L^{-1} is shown. As it is obvious from the inset of this figure, I_p (peak 1) increased linearly with growing analyte concentration and the obtained dependence can be described by the equation (7) with

the corresponding correlation coefficient. Calculated statistical parameters are summarized in Table 1. The obtained value of *LOD* is very low (5.9×10^{-8} mol L^{-1}), especially considering the use of bare BDDE as working electrode. Our method was also compared with those published for MLX determination in literature. As it is obvious from Table 2, best results were obtained using adsorptive stripping voltammetry in connection with HMDE [31] or with carbon paste electrode modified by molecularly imprinted polymer nanoparticle-multiwall carbon nanotubes (MIP@MWCNT/CPE) [36]. On the other hand, BDDE provide significantly better value of *LOD* than bulk CPE [33]. The main advantage of BDDE in comparison with other presented modified electrodes [34-37] lies in better repeatability and stability of the electrode surface as well as in simple and time undemanding preparation of the electrode for measurement.

$$I_p\ [\text{nA}] = (12.370 \pm 0.089)\ c\ [\mu\text{mol L}^{-1}] - (0.64 \pm 0.91),\ r = 0.9995 \quad (7)$$

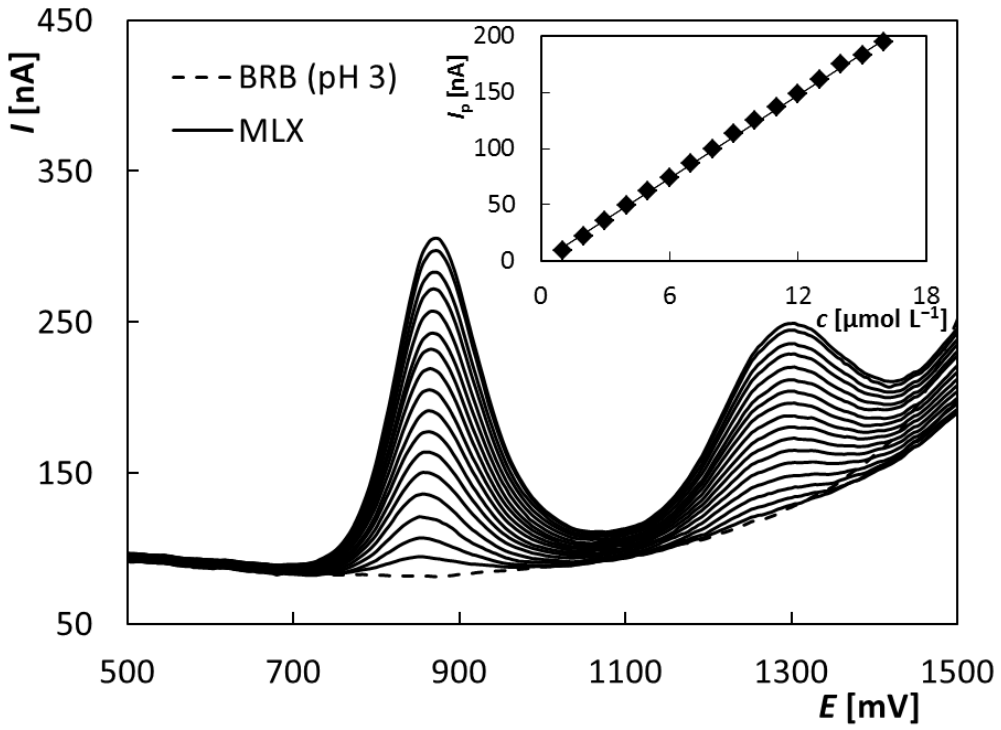

Figure 6 DPV voltammograms of MLX obtained on BDDE in dependence on concentration; supporting electrolyte – BRB (pH 3), E_{in} = 0 mV, E_{fin} = +2000 mV, v = 40 mV s^{-1}, pulse

height = +60 mV, pulse width = 30 ms, c_{MLX} = 1.0×10^{-6}-1.7×10^{-5} mol L^{-1}; ***Inset:*** Dependence of I_p on concentration of MLX.

Table 1 Statistical parameters for MLX determination

*LOD** [mol L^{-1}]	*LOQ** [mol L^{-1}]	*LDR* [mol L^{-1}]	RSD_{11}** [%]
5.9×10^{-8}	1.9×10^{-7}	2.5×10^{-7}-8.5×10^{-5}	0.3

*Calculated from the recorded concentration dependence in the range of 2.5×10^{-7}-1.25×10^{-6} mol L^{-1}, **calculated from the 11 repeated measurements at the concentration of MLX of 5.0×10^{-6} mol L^{-1}.

Table 2 Comparison of the obtained results with those published in literature

Method	Electrode	Electrolyte	LOD [mol L^{-1}]	Real sample	Ref.
SSOP	DME	AcB (pH 4.76)	3.0×10^{-8}*	tablets	29
DPP	DME	AcB (pH 4.88)	5.7×10^{-8}*	spiked plasma	30
CAS SWV	HMDE	AcB (pH 5.0)	2.0×10^{-11}*	spiked plasma	31
CAS DPV	HMDE	BRB (pH 4.0)	2.9×10^{-9}**	tablets	32
LSV	CPE	BRB (pH 3.0)	1.6×10^{-7}*	tablets	33
ASV	cysteic acid/GCE	BRB (pH 1.86)	1.9×10^{-9}*	tablets spiked plasma	34
DPV	PLL/GO-COOH/GCE	BRB (pH 3.0)	8.7×10^{-7}***	tablets spiked serum	35
AAS DPV	MIP@MWCNT/CPE	PB (pH 9.0)	9.2×10^{-11}**	spiked plasma	36
ASV	GR/CPE	BRB (pH 2)	2.6×10^{-9}***	tablets	37
DPV	BDDE	BRB (pH 3)	5.9×10^{-8}**	tablets	Pres.

AAS DPV – anodic adsorptive stripping differential pulse voltammetry, AcB – acetate buffer solution, ASV – adsorptive stripping voltammetry, BRB – Britton-Robinson buffer solution, CAS SWV – cathodic adsorptive stripping square wave voltammetry, CAS DPV – cathodic

adsorptive stripping differential pulse voltammetry, CPE – carbon paste electrode, cysteic acid/GCE – cysteic acid modified glassy carbon electrode, DME – dropping mercury electrode, DPP – differential pulse polarography, DPV – differential pulse voltammetry GR/CPE – graphene nanoparticles modified carbon paste electrode, HMDE – hanging mercury drop electrode, LSV – linear-scan voltammetry, MIP@MWCNT/CPE – carbon paste electrode modified by molecularly imprinted polymer nanoparticle-multiwall carbon nanotubes, PB – phosphate buffer solution, PLL/GO-COOH/GCE – poly-L-lysine/carboxylated graphene oxide modified glassy carbon electrode, SSOP – single sweep oscillopolarography
[*]calculated as a signal to noise ratio of 3, [**]calculated as 3× standard deviation of an intercept divided by a slope, [***]calculation procedure was not specified

Verification of the proposed method was realized by determining a known amount of an analyte in model solutions. Concentration of MLX in a polarographic vessel was 1.0×10^{-6} mol L^{-1} in 15 mL of BRB (pH 3) and standard addition method was applied. Always 2-3 standard additions of standard solution of MLX (V = 15 μL, c_{MLX} = 0.001 mol L^{-1}) were added. Analysis was 5× repeated and parameters like average value with confidence interval, recovery and *RSD* of repeated determination were calculated. The obtained results summarized in Table 3 suggest that DPV with BDDE allows accurate, correct, and repeatable results (RSD_5 = 2.11 %).

3.3.3. Analysis of pharmaceutical samples

Finally, the developed method for voltammetric determination of MLX using BDDE was applied in the analysis of the pharmaceutical preparation, namely drug in tablet form Meloxicam Mylan with the declared MLX content of 15 mg per tablet. The procedure of sample preparation and analysis by standard addition method is described in detail in the experimental part. The analysis was 5× repeated again and one example of the obtained voltammograms together with the graphical evaluation of standard addition method is shown in Fig 7. The appropriated statistical parameters as in case of model solutions are placed in Table 3. It can be concluded that the obtained average value (15.25±0.27) corresponds with

that declared by producer and the determination of MLX in complicate matrix is also very well repeatable (RSD_5 = 2.33).

Table 3 Repeated determination of MLX in model solutions and pharmaceutical preparation

	Added [mol L^{-1}]	Found [mol L^{-1}]	Recovery [%]	RSD_5 [%]
model solution	1.0×10^{-6}	$(0.981\pm0.014)\times10^{-6}$	97.2-101.1	2.11
	Declared [mg/Tbl]	Found [mg/Tbl]	Recovery [%]	RSD_5 [%]
Meloxicam Mylan	15	(15.25±0.27)	98.1-103.6	2.33

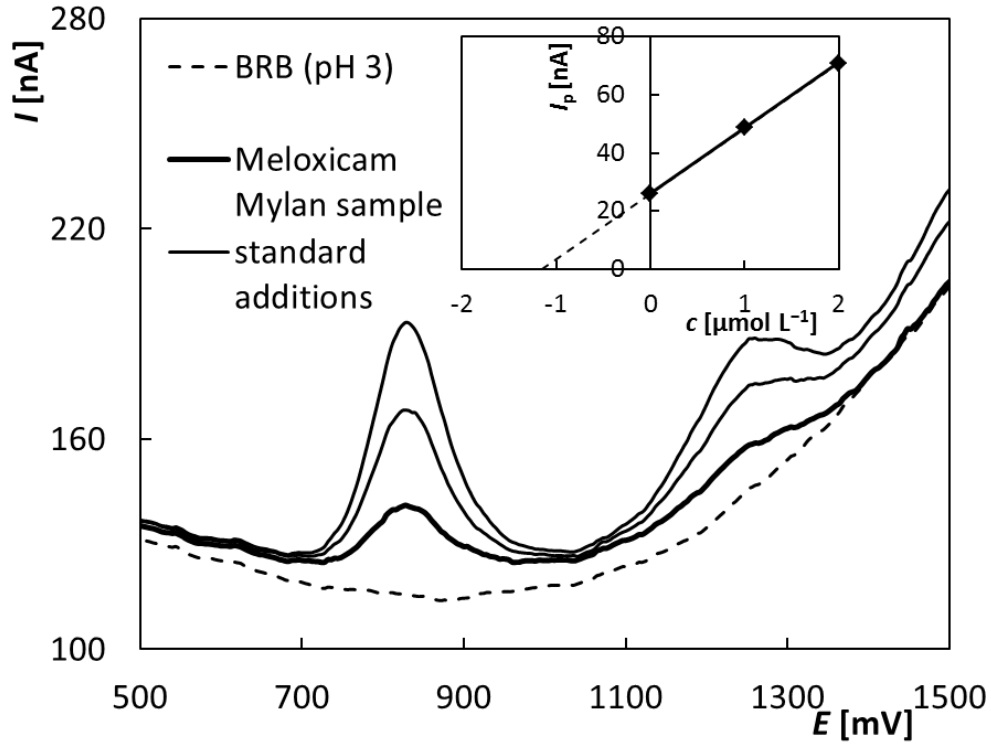

Figure 7 DPV voltammograms of analysis of pharmaceutical preparation "Meloxicam Mylan 15 mg" obtained on BDDE using standard addition method; supporting electrolyte – BRB (pH 3), E_{in} = 0 mV, E_{fin} = +2000 mV, v = 40 mV s^{-1}, pulse height = +60 mV, pulse width = 30 ms, standard additions – V = 15 µL, c_{MLX} = 0.001 mol L^{-1}; ***Inset:*** Graphical evaluation of standard addition method.

4 Conclusion

The electrochemical oxidation of a nonsteroidal anti-inflammatory drug meloxicam on BDDE proceeds in two irreversible voltammetric steps in wide pH range. Mechanism of the electrochemical oxidation was proposed and confirmed using high performance liquid chromatography/mass spectrometry analysis of MLX solutions electrolyzed on a carbon fiber brush electrode. Thiazole and benzoisothiazole were proved as the main reaction products of the first two-electron oxidation step. The second two-electron step includes probably subsequent oxidation of aldehyde group of thiazole to give the corresponding monoamide of oxalic acid.

Voltammetric method for MLX determination utilizing DPV in connection with BDDE was developed. The first anodic signal in BRB of pH 3 was found as optimum for analytical purposes and the basic parameters of DPV like scan rate, pulse height, and pulse width were optimized. The suitable BDDE pretreatment procedure was also suggested. The proposed method provides a wide *LDR* (2.5×10^{-7}-8.5×10^{-5} mol L^{-1}) and very low *LOD* (5.9×10^{-8} mol L^{-1}), which is significantly lower than that achieved for bulk CPE and comparable with those reported for various modified electrodes. Using model solutions, recovery of this method was ranging from 97.2-101.1 %. The applicability of the proposed method for practical samples was verified by successful analysis of pharmaceutical samples.

Acknowledgements This work was supported by the grant project of The Czech Science Foundation (project No. 17-03868S) and by The University of Pardubice (projects No. SGSFChT_2019_001).

References

[1] K. T. Olkkola, A. V. Brunetto, M. J. Mattila: Pharmacokinetics of oxicam nonsteroidal anti-inflammatory agents. Clin. Pharmacikinet. 26 (1994) 107-120.

[2] A. Barner: Review of clinical trials and benefit/risk ratio of meloxicam. Scand. J. Rheumatol. 25 (1996) 29-37.

[3] R. Fleischmann, I. Iqbal, G. Slobodin: Meloxicam. Expert Opin. Pharmacother. 3 (2002) 1501-1512.

[4] M. Ahmed, D. Khanna, D. E. Furst: Meloxicam in rheumatoid arthritis. Expert Opin. Drug Metab. Toxicol. 1 (2005) 739-751.

[5] C. J. Hawkey, J. Dequeker: Low gastrointestinal toxicity of meloxicam, a preferential inhibitor of the inducible cyclooxygenase (COX-2) enzyme compared to piroxicam. GUT 41 (1997) A7-A8.

[6] P. Staerkel, Y. Horsmans: Meloxicam-induced liver toxicity. Acta Gastro-Enterol. Belg. 62 (1999) 255-256.

[7] B. T. Villalba, F. R. Ianiski, A. G. Vogt, M. P. Pinz, A. S. Reis, R. A. Vaucher, M. P. Soares, E. A. Wilhelm, C. Luchese: Polymeric nanocapsules as a technological alternative to reduce the toxicity caused by meloxicam in mice. Regul. Toxicol. Pharmacol. 81 (2016) 316-321.

[8] E. Hoffman, D. M. Mladsi, B. Cryer, W. Hopkins, D. C. Brater, R. Parikh, R. Goyal, J. Castellsague, D. Stafkey-Mailey, C. Young: Dose-related risks of cardiovascular, gastrointestinal, and renal adverse events associated with meloxicam among patients with osteoarthritis: An observational study using US claims data. Arthritis Rheumatol. 68 (2016) 2359.

[9] K. Nakagawa, Y. Miyagawa, N. Takemura, H. Hirose: Influence of preemptive analgesia with meloxicam before resection of the unilateral mammary gland on postoperative cardiovascular parameters in dogs. J. Vet. Med. Sci. 69 (2007) 939-944.

[10] W. F. Huang, F. Y. Hsiao, Y. W. Tsai, Y. W. Wen, Y. T. Shih: Cardiovascular events associated with long-term use of celecoxib, rofecoxib and meloxicam in Taiwan - An observational study. Drug Saf. 29 (2006) 261-272.

[11] A. Mandi, M. Ahmad, M. Usman: New high performance liquid chromatographic method for simultaneous determination of diclofenac and meloxicam in oral formulation of liposomes and human plasma. J. Chem. Soc. Pak. 32 (2010) 654-661.

[12] A. Medvedovici, F. Albu, C. Georgita, C. Mircioiu, V. David: A non-extracting procedure for the determination of meloxicam in plasma samples by HPLC-diode array detection. Arzneimittelforschung-Drug Res. 55 (2005) 326-331.

[13] L. Leal, D. Bedor, E. Melo: Determination of meloxicam in human plasma administrated with four drugs by LC method: Application to a pilot bioavailability study. Lat. Am. J. Pharm. 30 (2011) 1883-1888.

[14] S. Cox, J. Bailey, M. White, K. Gordon, M. Souza: Determination of meloxicam in egg whites and yolks using reverse phase chromatography. J. Chromatogr. Sci. 55 (2017) 610-616.

[15] K. B. Liew, G. O. K. Loh, Y. T. F. Tan, K. K. Peh: Improved protein deproteinization method for the determination of meloxicam in human plasma and application in pharmacokinetic study. Biomed. Chromatogr. 28 (2014) 1782-1788.

[16] S. E. Vignaduzzo, P. M. Castellano, T. S. Kaufman: Method development and validation for the simultaneous determination of meloxicam and pridinol mesylate using RP-HPLC and its application in drug formulations. J. Pharm. Biomed. Anal. 46 (2008) 219-225.

[17] H. W. Lee, H. Y. JI, H. Y. KIM: Liquid chromatography-tandem mass spectrometry method for the determination of meloxicam and its metabolite 5-carboxymeloxicam in human plasma. Bioanal. 1 (2009) 63-70.

[18] Y. Z. Tian, X. Wu, M. J. Zhang, L. S. Zhao, Z. L. Xiong, F. Qin: Quantitative determination of meloxicam in dog plasma by high performance liquid chromatography-tandem mass spectrometry and its application in a pharmacokinetic study. Biomed. Chromatogr. 32 (2018) e4228.

[19] H. W. Lee, H. Y. Ji, H. Y. Kim, K. C. Lee, H. S. Lee: Liquid chromatography-tandem mass spectrometry method for the determination of meloxicam and its metabolite 5-carboxymeloxicam in human plasma. Bioanal. 1 (2009) 63-70.

[20] H. M. Rigato, G. D. Mendes, N. C. D. Borges, R. A. Moreno: Meloxicam determination in human plasma by high-performance liquid chromatography coupled with tandem mass spectrometry (LC-MS-MS) in Brazilian bioequivalence studies. Int. J. Clin. Pharmacol. Ther. 44 (2006) 489-498.

[21] M. Starek, J. Krzek: TLC determination of meloxicam in tablets and after acidic and alkaline hydrolysis. Acta Pol. Pharm. 69 (2012) 225-235.

[22] M. Mandrescu, A. F. Spac, V. Domeanu: Spectrophotometric determination of meloxicam. Rev. Chim. 60 (2009) 160-163.

[23] B. Gurupadaya, M. Trinath, K. Shilpa: Spectrophotometric determination of meloxicam by sodium nitroprusside and 1,10-phenanthroline reagents in bulk and its pharmaceutical formulation. Indian J. Chem. Technol. 20 (2013) 111-115.

[24] R. Rahmati, Z. Rafiee: A biocompatible high surface area ZnO-based molecularly imprinted polymer for the determination of meloxicam in water media and plasma. New J. Chem. 43 (2019) 8492-8501.

[25] V. Vasiliki, P. C. A. G. Pinto, M. L. M. F. S. Saraiva, J. L. F. C. Lima: Sequential injection determination of meloxicam in pharmaceutical formulations with spectrophotometric detection. Can. J. Anal. Sci. Spectrosc. 52 (2007) 351-358.

[26] E. M. Hassan: Spectrophotometric and fluorimetric methods for the determination of meloxicam in dosage forms. J. Pharm. Biomed. Anal. 27 (2002) 771-777.

[27] J. Tian, Ch. Li, L. Shaopu: A rapid and highly sensitive fluorimetric method for the determination of meloxicam using uranyl acetate, Anal. Methods. 6 (2014) 5221-5226.

[28] H. Y. Liu, L. Zhang, Y. H. Hao, Q. J. Wang, P. G. He, Y. Z. Fang: Flow-injection chemiluminescence determination of meloxicam by oxidation with N-bromosuccinimide. Anal. Chim. Acta 541 (2005) 187-192.

[29] H. Huang, H. Y. Gao, Y. H. Zeng: Single sweep oscillopolarography of meloxicam. Chin. J. Anal. Chem. 28 (2000) 1501-1503.

[30] S. Altinoz, E. Nemutlu, S. Kir: Polarographic behaviour of meloxicam and its determination in tablet preparations and spiked plasma. Farmaco 57 (2002) 463-468.

[31] A. E. Radi, M. Ghoneim, A. Beltagi: Cathodic adsorptive stripping square-wave voltammetry of the anti-inflammatory drug meloxicam. Chem. Pharm. Bull. 49 (2001) 1257-1260.

[32] A. M. Beltagi, M. M. Ghoneim, MM; A. Radi: Electrochemical reduction of meloxicam at mercury electrode and its determination in tablets. J. Phar. Biomed. Anal. 27 (2002) 795-801.

[33] A. Radi, M. A. El Ries, F. El-Anwar, Z. El-Sherif: Electrochemical oxidation of meloxicam and its determination in tablet dosage form. Anal. Lett. 34 (2001) 739-748.

[34] C. Y. Wang, Z. X. Wang, J. Guan, X. Y. Hu: Voltammetric determination of meloxicam in pharmaceutical formulation and human serum at glassy carbon electrode modified by cysteic acid formed by electrochemical oxidation of L-cysteine. Sensors 6 (2006) 1139-1152.

[35] S. Cheemalapati, B. Devadas, S. M. Chen: Novel poly-L-lysine/carboxyl-group enriched graphene oxide/modified electrode preparation, characterization and

applications for the electrochemical determination of meloxicam in pharmaceutical tablets and blood serum. Anal. Meth. 6 (2014) 8426-8434.

[36] S. Azodi-Deilami, E. Asadi, M. Abdouss, F. Ahmadi, A. H. Najafabadi, S. Farzaneh: Determination of meloxicam in plasma samples using a highly selective and sensitive voltammetric sensor based on carbon paste electrodes modified by molecularly imprinted polymer nanoparticle-multiwall carbon nanotubes. Anal. Meth. 7 (2015) 1280-1292.

[37] M. E. Eroglu, D. E. Bayraktepe, K. Polat, Z. Yazan: Electro-oxidation mechanism of meloxicam and electrochemical sensing platform based on graphene nanoparticles for its sensing pharmaceutical sample. Curr. Pharm. Anal. 15 (2019) 346-354.

[38] M. Iwaki, S. Sato, K. Takahashi, H. Sakairi: Electrical conductivity of nitrogen and argon implanted diamond. Nucl. Instr. Meth. 209 (1983) 1129-1133.

[39] Y. V. Pleskov, A. Y. Sakharova, M. D. Krotova, L. L. Bouilov, B. V. Spitsyn: Photoelectrochemical properties of semiconductor diamond. J. Electroanal. Chem. Interfac. Electrochem. 228 (1987) 19-27.

[40] K. Patel, K. Hashimoto, A. Fujishima: Application of boron-doped CVD-diamond film to photoelectrode. Denki Kagaku 60 (1992) 659-661.

[41] K. Patel, K. Hashimoto, A. Fujishima: Photoelectrochemical investigations on boron-doped chemically vapor-deposited diamond electrodes. J. Photochem. Photobiol. A: Chem. 65 (1992) 419-429.

[42] G. M. Swain, R. Ramesham: The electrochemical aktivity of boron-doped polycrystalline diamond thin film electrodes Anal. Chem. 65 (1993) 345-351.

[43] J. Xu, M. C. Granger, Q. Chen, J. W. Strojek, T. E. Lister, G. M. Swain: Boron-doped diamond thin-film electrodes. Anal. Chem. New Feat. 1 (1997) 591-597.

[44] R. G. Compton, J. S. Foord, F. Marken: Electroanalysis at diamond-like and doped-diamond electrodes. Electroanal. 15 (2003) 1349-1363.

[45] K. Peckova, J. Musilova, J. Barek: Boron-doped diamond film electrodes-New tool for voltammetric determination of organic compounds. Crit. Rev. Anal. Chem. 39 (2009) 148-172.

[46] J. H. T. Luong, K. B. Male, J. D. Glennon: Boron-doped diamond electrode: synthesis, characterization, functionalization, and analytical application. Analyst 134 (2009) 1965-1979.

[47] R. Selesovska, M. Stepankova, L. Janikova, K. Novaková, M. Vojs, M. Marton, M. Behul: Surface and electrochemical characterization of boron-doped diamond electrodes prepared under different conditions. Monatsh. Chem. 147 (2016) 1353-1364.

[48] K. Schwarzova-Peckova, J. Vosáhlova, J. Barek, I. Sloufova, E. Pavlova, V. Petrak, J. Zavazalova: Influence of boron content on the morphological, spectral, and electroanalytical characteristics of anodically oxidized boron-doped diamond electrodes. Electrochim. Acta 243 (2017) 170-182.

[49] R. Selesovska, B. Krankova, M. Stepankova, P. Martinkova, L. Janikova, J. Chylkova, M. Vojs: Influence of boron content on electrochemical properties of boron-doped diamond electrodes and their utilization for leucovorin determination. J. Electroanal. Chem. 821 (2018) 2-9.

[50] J. M. Freitas, T. D. Oliveira, R. A. A. Munoz, E. M. Richter: Boron-doped diamond electrodes in flow-based systems. Front. Chem. 7 (2019) No. 190.

[51] N. J. Yang, S. Y. Yu, J. V. Macpherson, Y. Einaga, H. Y. Zhao, G. H. Zhao, G. Swain, X. Jiang: Conductive diamond: synthesis, properties, and alectroanalytical applications. Chem. Soc. Rev. 48 (2019) 157-204.

[52] S. Baluchová, A. Daňhel, H. Dejmková, V. Ostatná, M. Fojta, K. Schwarzová-Pecková: Recent progress in the applications of boron doped diamond electrodes in electroanalysis of organic compounds and biomoleculs – A review. Anal. Chim. Acta 1077 (2019) 30-66.

[53] R. Selesovska, L. Janikova-Bandzuchova, J. Chylkova: Sensitive voltammetric sensor based on boron-doped diamond electrode for determination of the chemotherapeutic drug methotrexate in pharmaceutical and biological samples. Electroanalysis 27 (2015) 42-51.

[54] D. M. Stankovic, K. Katcher: The immunosuppressive drug - rapamycin - electroanalytical sensing using boron-doped diamond electrode. Electrochim. Acta 168 (2015) 76-81.

[55] M. Brycht, K. Kaczmarska, B. Uslu, S. A. Ozkan, S. Skrzypek: Sensitive determination of anticancer drug imatinib in spiked human urine samples by differential pulse voltammetry on anodically pretreated boron-doped diamond electrode. Diam. Rel. Mat. 68 (2016) 13-22.

[56] L. Svorc, K. Borovska, K. Cinkova, D. M. Stankovic, A. Plankova: Advanced electrochemical platform for determination of cytostatic drug flutamide in various matrices using a boron-doped diamond electrode. Electrochim. Acta 251 (2017) 621-630.

[57] R. Selesovska, B. Krankova, M. Stepankova, P. Martinkova, L. Janikova, J. Chylkova, T. Navratil: Voltammetric determination of leucovorin in pharmaceutical preparations using a boron-doped diamond electrode. Monatsh. Chem. 149 (2018) 1701-1708.

[58] M. Stepankova, R. Selesovska, L. Janikova, P. Martinkova, M. Marton, P. Michniak, J. Chylkova: Comparison of application options of boron-doped diamond electrodes with

various boron content for the determination of bioactive organic compounds. Chem. Listy 112 (2018) 389-395.

[59] S. Seyidahmet, F. Donmez, Y. Yardim, Z. Senturk: Simple, rapid, and sensitive electrochemical determination of antithyroid drug methimazole using a boron-doped diamond electrode. J. Iran. Chem. Soc. 16 (2019) 913-920.

[60] J. Skopalova, P. Bartak, P. Bednar, H. Tomkova, T. Ingr, I. Lorencova, P. Kucerova, R. Papousek, L. Borovcova, K. Lemr: Carbon fiber brush electrode as a novel substrate for atmospheric solids analysis probe (ASAP) mass spectrometry: Electrochemical oxidation of brominated phenols. Anal. Chim. Acta 999 (2018) 60-68.

[61] R. Jerga, V. Müllerová, J. Štěpánková, P. Barták, H. Tomková, J. Rozsypal, J. Skopalová: Phospholipid‐modified carbon fiber brush electrode for the detection of dopamine and 3,4‐dihydroxyphenylacetic acid. Monatsh. Chem. 150 (2019) 395-400.

[62] B. Bozal, B. Uslu: Applications of carbon based electrodes for voltammetric determination of lornoxicam in pharmaceutical dosage form and human serum. Comb. Chem. High T. Scr. 13 (2010) 599-609.

[63] A. A. J. Torriero, C. E. Tonn, L. Sereno, J. Raba: Electrooxidation mechanism of non-steroidal anti-inflammatory drug piroxicam at glassy carbon electrode. J. Electroanal. Chem. 588 (2006) 218-225.

[64] P. Luger, K. Daneck, W. Engel, G. Trummlitz, K. Wagner: Structure and physicochemical properties of meloxicam, a new NSAID. Eur. J. Pharm. Sci. 4 (1996) 175-187.

[65] S. Treimer, A. Tang, D. C. Johnson: A Consideration of the application of Koutecky-Levich plots in the diagnoses of charge-transfer mechanisms at rotated disk electrodes. Electroanalysis 14 (2002) 165-171.

[66] C. R. Wilke, P. Chang: Correlation of diffusion coefficients in dilute solutions. AIChE J. 1 (1955) 264-270.

[67] G. P. Cunningham, G. A. Vidulich, R. L. Kay: Several properties of acetonitrile-water, acetonitrile-methanol, and ethylene carbonate-water system: J. Chem. Eng. Data 12 (1967) 336-337.

[68] P. Kucerova, J. Skopalova, L. Kucera, J. Hrbac, K. Lemr: Electrochemical oxidation of fesoterodine and identification of its oxidation products using liquid chromatography and mass spectrometry. Electrochim. Acta 159 (2015) 131–139.

[69] A. T. Åberg, C. Olsson, U. Bondesson, M. Hedeland, A mass spectrometric study on meloxicam metabolism in horses and the fungus *Cunninghamella elegans*, and the relevance of this microbial system as a model of drug metabolism in the horse. J. Mass Spectrom. 44 (2009) 1026-1037.

[70] C. S. H. Jesus, V. C. Diculescu: Redox mechanism, spectrophotometrical characterisation and voltammetric determination in serum samples of kinases inhibitor and anticancer drug dasatinib. J. Electroanal. Chem. 752 (2015) 47-53.

[71] J. V. Macpherson: A practical guide to using boron doped diamond in electrochemical research. Phys. Chem. Chem. Phys. 17 (2015) 2935-2949.

Supplemental material for on-line publication only

Click here to download Supplemental material for on-line publication only: Supplementary material 1.docx

Declaration of Interest Statement

- Electrochemical behavior of a nonsteroidal anti-inflammatory drug meloxicam (MLX) was firstly studied using boron doped diamond electrode.
- Mechanism of the electrochemical oxidation was proposed and supported with high performance liquid chromatography/mass spectrometry analysis of electrolyzed meloxicam solutions.
- Sensitive voltammetric method for MLX determination was developed.
- New developed method was successfully applied for pharmaceutical samples analysis.

Author Contributions Section

Renáta Šelešovská – work organization, voltammetric analysis, data evaluation, article writing

Frederika Hlobeňová – voltammetric analysis

Jana Skopalová – GC-MS analysis, GC-MS spectra interpretation, article writing

Petr Cankař – GC-MS spectra interpretation

Lenka Janíková – literary research, data evaluation

Jaromíra Chýlková – voltammetric analysis